

THE NON-UNIFORM ARGON DC GLOW DISCHARGE SYSTEM PARAMETERS  
MEASURED WITH FAST THREE COUPLES OF DOUBLE PROBE

A THESIS SUBMITTED TO  
THE GRADUATE SCHOOL OF NATURAL AND APPLIED SCIENCES  
OF  
MIDDLE EAST TECHNICAL UNIVERSITY

BY

DEMIRAL AKBAR

IN PARTIAL FULFILLMENT OF THE REQUIREMENTS  
FOR  
THE DEGREE OF DOCTOR OF PHILOSOPHY  
IN  
PHYSICS

MARCH 2006

Approval of the Graduate School of Natural and Applied Sciences.

---

Prof. Dr. Canan Özgen  
Director

I certify that this thesis satisfies all the requirements as a thesis for the degree of Doctor of Philosophy.

---

Prof. Dr. Sinan Bilikmen  
Head of Department

This is to certify that we have read this thesis and that in our opinion it is fully adequate, in scope and quality, as a thesis for the degree of Doctor of Philosophy.

---

Prof. Dr. Sinan Bilikmen  
Supervisor

Examining Committee Members

Prof. Dr. Gülay Öke (METU, PHYS) \_\_\_\_\_

Prof. Dr. Sinan Bilikmen (METU, PHYS) \_\_\_\_\_

Prof. Dr. Cevdet Tezcan (Başkent Univ., ENGINE.) \_\_\_\_\_

Assoc. Dr. Serhat Çakır (METU, PHYS) \_\_\_\_\_

Assoc. Prof. Akif Esendemir (METU, PHYS) \_\_\_\_\_

“I hereby declare that all information in this document has been obtained and presented in accordance with academic rules and ethical conduct. I also declare that, as required by these rules and conduct, I have fully cited and referenced all material and results that are not original to this work.”

Name Surname : DEMIRAL AKBAR

Signature :

## ABSTRACT

### THE NON-UNIFORM ARGON DC GLOW DISCHARGE SYSTEM PARAMETERS MEASURED WITH FAST THREE COUPLES OF DOUBLE PROBE

Akbar, Demiral

Ph.D., Department of Physics

Supervisor: Prof. Dr. Sinan Bilikmen

March 2006, 80 pages.

The non-uniform dc glow discharge plasma system is studied by using isolated computer controlled three couples of double probe system (TCDP) in argon gas, simultaneously. TCDP system has been developed to use for magnetized, unmagnetized, and for low oscillating plasma systems by using low pass filter with optically isolated circuitry to minimize the measurement errors with higher resolution and accuracy. Difference in the shapes and diameters of the discharge tube from region to region leads to change in the positive column glow discharge properties. This is because the positive column inhomogeneities, rising from the increase in the electron densities at the small tube radius region than the large one. Therefore, the axial electric field and the electron temperature have been diverted from their normal behavior in the positive column. However, at the large radius regions, the axial electric field seems to stay approximately constant at higher discharge currents.

On the other hand, In this work the radial dependence of the electron temperature, density, floating potential, and the normalized probe radius ( $\xi = r_p/\lambda_D$ ) has been investigated. Since, the probe radius is smaller than Debye length, the orbital motion limited (OML) theory has been used. As a result, the electron temperature (at the center) decreased and density increased with decreasing tube radius, and they have maximum values at the first probe (near the cathode). The electron density  $n_e$  was observed to decrease and electron temperature  $T_e$  to increase with increasing the discharge current. The floating potential has less negative value with decreasing tube radius except at the higher currents. Finally, it has been found that the  $\xi$  is proportional with electron density, but it remains constant depending on the value of  $T_e$  and  $n_e$ .

Keywords: Fast Langmuir probe, electron temperature, electron density, positive column, electric field, floating potential, Debye length.

## ÖZ

### DÜZGÜN OLMİYAN ARGON DC PLAZMA BOŞALMA SİSTEMİNDEKİ PARAMETRELERİN HIZLI ÜÇ ÇİFT İKİLİ PROB İLE ÖLÇÜLMESİ

Akbar, Demiral

Doktora, Fizik Bölümü

Tez Yöneticisi: Prof. Dr. Sinan Bilikmen

Mart 2006, 80 sayfa.

Argon ortamında çalışan izole bilgisayar kontrollü üç çift, ikili prob sistemi kullanılarak düzgün olmayan dc boşalmalı plazma sistemi çalışılmıştır. Düşük geçiş filtrelili optiksel izole edilmiş elektronik devrelerin kullanıldığı (ÜÇİP) sistemi manyetik, manyetik olmayan, ve düşük salınımlı plazma sistemlerinde ölçüm hatalarını en aza indirmek için geliştirildi. Plazma tüpü bölgeden bölgeye değişen yapısı ve yarıçapı pozitif kolon özelliklerinin değişmesine neden olmuştur. Bunun sebebi, küçük yarıçaplı bölgedeki elektron yoğunluğunun büyük yarıçaplı bölgeye göre daha fazla artması nedeniyle pozitif kolonun homojen olmamasıdır. Bu nedenle aksel elektrik alanı ve elektron sıcaklığı normal alışlagelmiş sistemlerdeki davranışından farklı olmuştur. Ancak, büyük çaplı bölgelerde, yüksek boşaltım akımında aksel elektrik alanının yaklaşık olarak sabit kaldığı görülmüştür.

Diğer taraftan bu araştırmada , elektron sıcaklığı, yoğunluğu, yalıtılmış potansiyel , ve normalize edilmiş prob yarıçapının ( $\xi = r_p/\lambda_D$ ) ışınal doğrultuya bağlı

arařtırılmıřtır. Prob yarıçapı, Debye uzunluęundan küçük olduęu için sınırlı yörüngesel hareket (SYH) teorisi kullanılmıřtır. Sonuç olarak, elektron sıcaklıęı (merkezde) azalmıř ve elektron yoęunluęu, tüp yarıçapı azaldıkça artmıřtır, ve ilk propta (katod tarafında) elektron sıcaklıęı ve yoęunluęu maksimum olmuřtur. Bořalma akımının yükselmesiyle elektron yoęunluęunda ( $n_e$ ) azalma , elektron sıcaklıęında ( $T_e$ ) artıř gözlenmiřtir. Yüksek akımlar dıřında, tüp çapı azaldıkça, yalıtılmıř potansiyel daha negatif olmuřtur. Son olarak,  $\xi$ ' nin elektron yoęunluęu ile orantılı olduęu bulunmuřtur, fakat  $T_e$  ve  $n_e$  deęerlerine baęlı olarak  $\xi$  sabit kalmaktadır.

Anahtar Kelimeler: Hızlı Langmuir prob, elektron sıcaklıęı, elektron yoęunluęu, pozitif kolon, elektrik alanı, yalıtılmıř potansiyel, Debye uzunluęu.

...TO MY FAMILY



## ACKNOWLEDGMENTS

I am grateful to all who have helped me to have the opportunity and possibility to continue the graduate study and to prepare this thesis for home space dose not permit identification in this listing.

My sincere gratitude and deep appreciation to Prof. Dr. Sinan Bilikmen for his kind assistance and supervision.

I wish to thanks all staff of electronic laboratory and to my graduate friends, and with special thanks to TÜRKMEN ELI KÜLTÜR MERKEZİ.

## TABLE OF CONTENTS

PLAGIARISM . . . . .	iii
ABSTRACT . . . . .	iv
ÖZ . . . . .	vi
DEDICATION . . . . .	viii
ACKNOWLEDGMENTS . . . . .	viii
TABLE OF CONTENTS . . . . .	x
LIST OF TABLES . . . . .	xii
LIST OF FIGURES . . . . .	xiii
1 INTRODUCTION . . . . .	1
2 DC GLOW DISCHARGE . . . . .	5
2.1 Introduction . . . . .	5
2.2 General Characterization of DC Glow Discharges . . . . .	6
2.3 Positive Column . . . . .	14
2.4 Theory of Positive column . . . . .	17
3 ELECTRICAL LANGMUIR PROBE . . . . .	24
3.1 Overview of Langmuir Probes . . . . .	24
3.2 Probe Theory . . . . .	25
3.3 Electrical Probe at Low Pressure Discharge . . . . .	27
3.3.1 Single Probe . . . . .	27

	3.3.2	Double Probe . . . . .	28
4		EXPERIMENTAL APPARATUS . . . . .	38
	4.1	Discharge Tube and Double Probe System . . . . .	38
	4.2	The Pressure Measurement System . . . . .	45
5		RESULTS AND DISCUSSION . . . . .	46
	5.1	Double Probe Characteristics at Different Pressures and Constant Distance from The Axis: . . . . .	46
	5.1.1	Current-Voltage Characteristics: . . . . .	46
	5.1.2	The Electron Temperature and Density . . . . .	49
	5.1.3	The Electric Field . . . . .	53
	5.2	Double Probe Characteristics at Constant Pressure (0.7 torr) and Different Distances from The Axis: . . . . .	57
	5.2.1	Current-Voltage Characteristics: . . . . .	57
	5.2.2	The Electron Temperature and Density: . . . . .	60
	5.2.3	The Floating Potential (Radial Potential): . . . . .	64
	5.2.4	The Normalized Probe Radius $\xi = r_P/\lambda_D$ : . . . . .	66
6		CONCLUSION AND FUTURE WORKS . . . . .	71
	6.1	Conclusion . . . . .	71
	6.1.1	Conclusion For Axial Measurements . . . . .	71
	6.1.2	Conclusion For Radial Measurements . . . . .	73
	6.2	Future Works . . . . .	74
		REFERENCES . . . . .	75

## LIST OF TABLES

- 6.1 Electron temperatures  $T_e$ , electron densities  $n_e$ , and axial electric field  $E$  for all probes at different discharge currents. Note: numbers (1, 2, 3) refers to probe1, probe2, and probe3 respectively. . . . . 73

## LIST OF FIGURES

2.1	Classification of the glow discharge [4]. . . . .	9
2.2	Circuit used to establish glow discharge [10]. . . . .	11
2.3	Schematic V-I curve of a glow discharge [4]. . . . .	13
3.1	Electrical circuit for double probe measurement. . . . .	29
3.2	Characteristic of symmetric double probe. . . . .	30
3.3	Double probe potential:(a)Floating potential, no current through the probes; (b) Left-hand probe is strongly negative, and receives ionic saturation current.(c) Polarity reversal; the right-hand probe is strongly negative[4]. . . . .	31
4.1	Schematic diagram of experimental apparatus. . . . .	39
4.2	Schematic diagram of the double probe diagnostic system. . . . .	41
4.3	Floating Langmuir probe derive and current amplifier. . . . .	42
4.4	Floating Langmuir probe derive and current amplifier. . . . .	43
4.5	The electronic parts of the isolated computer controlled three couples of double probe (TCDP) system. . . . .	44
5.1	Double probe characteristic in argon gas at $I_d = 5$ mA (at fixed radial distance (1.7 cm), and (1 cm) for probes 1, 3 and 2 respectively), and different pressures. . . . .	47
5.2	Double probe characteristic in argon gas at $I_d = 15$ mA (at fixed radial distance (1.7 cm), and (1 cm) for probes 1, 3 and 2 respectively), and different pressures. . . . .	48
5.3	The experimental (symbols) and theoretical (lines) I-V curves for probes (P1-continuous, P2-dash, and P3- dots, for all figures) at discharge current $I_d=10$ mA and pressure 0.33 torr at fixed radial distance (1.7 cm), and (1 cm) for probes 1, 3 and 2 respectively. . . . .	49

5.4	Electron temperature as a function of $pR$ at discharge current (a) $I_d = 5$ mA, (b) $I_d = 10$ mA, and (c) $I_d = 15$ mA , at fixed radial distance (1.7 cm), and (1 cm) for probes 1, 3 and 2 respectively. . . . .	50
5.5	Electron density as a function of $pR$ at discharge current (a) $I_d = 5$ mA, (b) $I_d = 10$ mA, and (c) $I_d = 15$ mA , at fixed radial distance (1.7 cm), and (1 cm) for probes 1, 3 and 2 respectively. . . . .	52
5.6	Axial electric field as a function of $pR$ at discharge current (a) $I_d = 5$ mA, (b) $I_d = 10$ mA, and (c) $I_d = 15$ mA , at fixed radial distance (1.7 cm), and (1 cm) for probes 1, 3 and 2 respectively. . . . .	54
5.7	Electron temperature as a function of the axial electric field at discharge current (a) $I_d = 5$ mA, (b) $I_d = 10$ mA, and (c) $I_d = 15$ mA , at fixed radial distance (1.7 cm), and (1 cm) for probes 1, 3 and 2 respectively. . . . .	56
5.8	Double probe characteristic in argon gas at $I_d = 5$ mA at constant pressure ( $p = 0.7$ torr) and different distances. . . . .	58
5.9	Double probe characteristic in argon gas at $I_d = 15$ mA at constant pressure ( $p = 0.7$ torr) and different distances. . . . .	59
5.10	Electron temperature as a function of the different radial distance $R$ at discharge current (a) $I_d = 5$ mA, (b) $I_d = 10$ mA, and (c) $I_d = 15$ mA , at $P = 0.7$ torr. The experimental (symbols) and theoretical (lines) curves for probes (1-continuous, 2-dash, and 3-dots, for all figures). . . . .	61
5.11	Electron density as a function of the different radial distance $R$ at discharge current (a) $I_d = 5$ mA, (b) $I_d = 10$ mA, and (c) $I_d = 15$ mA , at $P = 0.7$ torr. . . . .	62
5.12	Floating potential as a function of the different radial distance $R$ at discharge current (a) $I_d = 5$ mA, (b) $I_d = 10$ mA, and (c) $I_d = 15$ mA, at $P = 0.7$ torr. . . . .	65
5.13	Radial variation of normalized probe radius $\xi$ as a function of electron temperature and density at discharge current $I_d = 5$ mA, and $P = 0.7$ torr. . . . .	68
5.14	Radial variation of normalized probe radius $\xi$ as a function of electron temperature and density at discharge current $I_d = 10$ mA, and $P = 0.7$ torr. . . . .	69

5.15 Radial variation of normalized probe radius $\xi$ as a function of electron temperature and density at discharge current $I_d = 15$ mA, and $P = 0.7$ torr. . . . .	70
--	----

## CHAPTER 1

### INTRODUCTION

DC glow discharge plasmas have been used for plasma processing applications in the low and intermediate pressure regimes in modern technology. During the last half century, low-temperature plasmas have made a dramatic impact on society, significantly improved the quality of life, and provided challenging scientific problems. Examples are the fluorescent lights, high-power switches that control the electrical grid and divert electrical power on command, gas discharge lasers, including the red He-Ne laser, and the high-power, infrared,  $CO_2$  lasers that are used daily in surgery and metal working, and plasma sources that provide positive and negative ions for ion-beam accelerators. Provided the opportunity, the field of low-temperature plasmas will continue to make significant contributions. The purity of the gas is often important, and the physics and chemistry of the excited atomic states dominate the discharge characteristics. In industrial applications, the stability of the discharge frequently impacts the design and utility of the process, and the heterogeneous wall chemistry often impacts its reproducibility and reliability.



Operation of plasmas in applications ranging from lasers to materials processing and lighting requires optimization of the temperatures and densities of these species. Scientists modeling these systems require a broader range of diagnostics to characterize species densities in benchmark plasmas, and more powerful methods for measuring and calculating. Using modern experimental and modeling techniques, the information of the positive column of dc metal-vapor rare-gas discharges was updated[1].

Despite problems of intrusion, contamination, and interpretation, the most widely used plasma diagnostic is the electrostatic probe. Each of these problems can be overcome at least partially, and probes provide useful estimates for electron and ion densities and the electron energy distribution function. For low-density discharges most often used in electronics materials processing, the electrostatic probe is the only method available. Careful and fast double probe measurements have been used to test theories of dc glow discharge of non-uniform system.

The influence of passive, i.e., not biased or powered, surfaces on processing in both low- and high-pressure discharges is widely recognized. But our current level of understanding is severely limited because these are inherently multidimensional effects and because the surfaces are poorly characterized. For low-pressure discharges, such surfaces are usually constructed of glass, quartz, alumina, stainless steel, or aluminum. Their behavior is often determined by exposure to energetic

electrons, ions, and photons and is reasonably well characterized for clean surfaces. However, when these surfaces are coated with plasma process products, their behavior is difficult or impossible to predict with our present knowledge and diagnostic capabilities.

In the past 10 years, experimental physics has benefited greatly from advances in digital technology. Analog-to-digital converters and microprocessors have decreased drastically in price. This system would permit the study of nonuniform and fully three dimensional plasma phenomena and plasma processes occurring on more than one spatial scale with unprecedented spatial and temporal resolution[2].

To measure plasma parameters, specially ion currents, with good accuracy and without contamination problems, it would be appropriated if the data collection can be done in a few seconds. The characteristic of the double Langmuir probe has been measured by developing fast computerized three couples of double probe system(TCDP). The data acquisition and control of the experiment is accomplished using input/output data acquisition/control board (NI 6014) from National Instruments connected to a personal computer (PC). The maximum time resolution of the system is ( $5 \mu s$ ).

In this study, a double Langmuir probes system was used instead of the single Langmuir probe. The reason for choosing the double Langmuir probes is that the floating circuitry does not require the presence of a grounded reference in

contact with the plasma. Also, the sampling current to the double probe is a small fraction of that drawing by a single probe, resulting in less perturbation in the plasma. Furthermore, an advantage of the double probes is that the total collected current cannot exceed the ion saturation current, thus localized distribution of plasma properties induced by the probe are minimal. The primary disadvantage is that double probe samples only the higher energy electrons, and not the bulk of electron distribution. Consequently, the electron temperature is expected to be overestimated. However, the contribution of the double Langmuir probes measurement is to provide a relatively quantitative tools to identify the electron distribution behavior. This tendency of electron distribution is valuable to understand the dc glow discharge processes [3].

## CHAPTER 2

### DC GLOW DISCHARGE

#### 2.1 Introduction

The glow discharge is a *self-sustaining* discharge with a *cold cathode* emitting electrons due to secondary emission mostly due to the ion bombardment. A distinctive feature of this discharge is a layer of large positive space charge at the cathode, with a strong field at the surface and considerable potential drop of 100-400 V (or more). This drop is known as *cathode fall*, and the thickness of the cathode fall layer is inversely proportional to the density ( pressure ) of the gas. If the inter-electrode separation is sufficiently large, an *electrically neutral* plasma region with fairly weak field is formed between the cathode layer and the anode. Its relatively homogenous middle part is called *positive column*. It is separated from the anode by the anode layer. The positive column of a dc glow discharge is the best pronounced and most widespread example of *weakly ionized non-equilibrium plasma* sustained by an electric field. In contrast to the cathode layer, whose existence is vital for the glow discharge, the positive column is not an essential part. No such column is formed if the cathode layer fills the

inter-electrode gap. If, however, the distance is sufficient for the formation of the required cathode layer, the glow discharge can not be ignited [4].

Studies of the different radius discharge tubes (e.g. narrow, capillary, rectangular, and cylindrical) positive column, and the comparison between this kind of vessels have been investigated separately by numerous authors[5, 6, 7, 8]. However, the investigations of the plasma parameters with variable tube radii in the same system and conditions have not been tested experimentally until now.

In many uniform dc glow discharge systems[9, 10, 11, 12], the electron density was small near the cathode and increased towards the anode, which is due to the ionization of electrons. On the other hand, electron temperature was increased sharply near the cathode, but decreased after negative glow, and extended and remained constant near the anode. In addition, the axial component of the electric field in the uniform positive column is found to be constant.

## 2.2 General Characterization of DC Glow Discharges

Since the electric discharge was established under the condition of pressure and current to form a glow discharge, the luminosity distribution can be shown schematically by Fig.(2.1).

In front of the cathode is very short dark space "Aston dark space", next to this there is the "cathode glow" whose length depends on the nature of the gas and its pressure. Following the cathode glow there is the "cathode dark space" the

cathode dark space is followed by the brightest of the glowing regions, called the "negative glow". The "Faraday dark space" follows the negative glow and in turn is followed by "positive column" which fills most of the length of the discharge tube. As the pressure decreases, the negative glow and the Faraday dark space may expand at the expense of the positive column which may disappear.

The positive column contracts radially as the pressure increases. At the anode there may or may not be a bright glow "anode glow" and a dark region "anode dark space", depending on the gas and on the value of the discharge current. The relative light intensities of the various region are shown in Fig.(2.1a).

The discharge is maintained by electrons produced at the cathode by positive-ion bombardment. In the Aston dark space there is an accumulation of these electrons which gain energy through cathode dark space. The cathode glow results from the decay of excitation energy of the positive ions on neutralization. When electrons gain sufficient energy in the cathode dark space to produce inelastic collisions, the excitation of the gas produces the negative glow. The end of the negative glow corresponds to the range of electrons with sufficient energy to produce excitation and in the Faraday dark space the electrons once more gain energy.

The positive column is the ionized region that extends from Faraday dark space almost to the anode dark space. It is not an essential part of the discharge, and for very short tubes the anode dark space is absent. In long tubes it serves as

a conducting path for the current. In the last few mean free path, the electrons may gain a high enough average energy to excite more freely as the positive ions are forced away from the anode. This produces the anode glow.

The distribution of the applied voltage along the glow discharge is shown in Fig.(2.1b). Three parts in the discharge may be distinguished, a cathode fall, an anode fall and a part where the electric field ( $E$ ) is constant "positive column". Most of the applied potential is required for the cathode dark space when the field strength is high as indicated in Fig.(2.1c).

The discharge current is mainly electronic rather than ionic because of the greater mobility of the electrons. The the current density and net charge density distribution along the discharge are shown in Fig.(2-1d and e) respectively[13].

As the pressure increases, all layers become thinner and shift to the closer to the cathode. A more extended faraday dark space can be distinguished; the rest of the tube or channel is occupied by the positive column. An elevated pressure causes the column to *contract* to the axis, while at low pressures the cross section of the tube is filled with the column in a *diffusion* manner [4].

Gases in the normal state are non-conducting. In order to set up "electrical discharges in gases" charge carriers have to be generated either in the gas volume or at the gas-electrode (or wall) interfaces. Therefore we have to discuss the processes responsible:

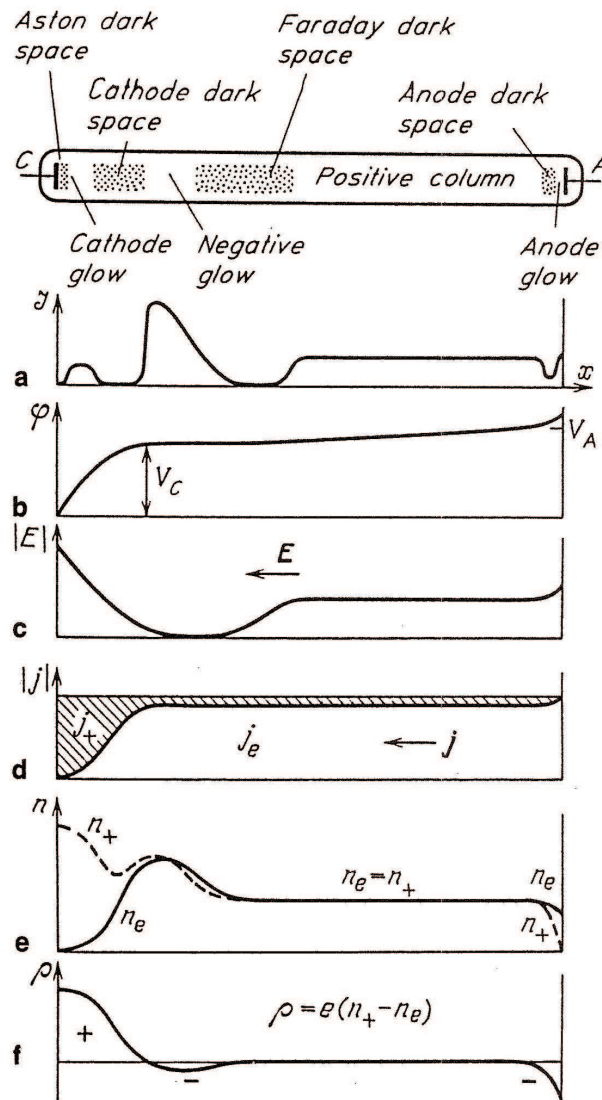


Figure 2.1: Classification of the glow discharge [4].



- 1- For the generation of charge carriers.
- 2- For their destruction or loss.
- 3- For their transport.

In particular, we have to consider these processes in the presence of an electric field  $E$ . It has been useful to distinguish two types of discharges: "Non-self sustained" discharge (e.g. ionization chambers) which rely for their existence on the supply of charge carriers by some external means, e.g. electron sources, X-rays, or more generally on "foreign" current. And "self sustained" discharges for which external currents are not needed. For both types the experimental arrangement is very simple Fig.(2.2).

We apply a variable voltage  $V$  between plane electrodes in a gas at a pressure  $p$  and measure the electrical current; charge carriers are supplied e.g. by irradiation of the gas volume with photons of sufficiently high energy. For the description of the discharge we may distinguish two strongly different situations:

- 1- At low current densities (i.e. charge carrier densities) the electric field will be uniform and is given by  $V/d$ , where  $d$  is the electrode distance.
- 2- At high current densities the electric field due to the space charge will become important and as a result the total electric field will be non-uniform. The electric field distribution has to be calculated by means of Poisson's equation:

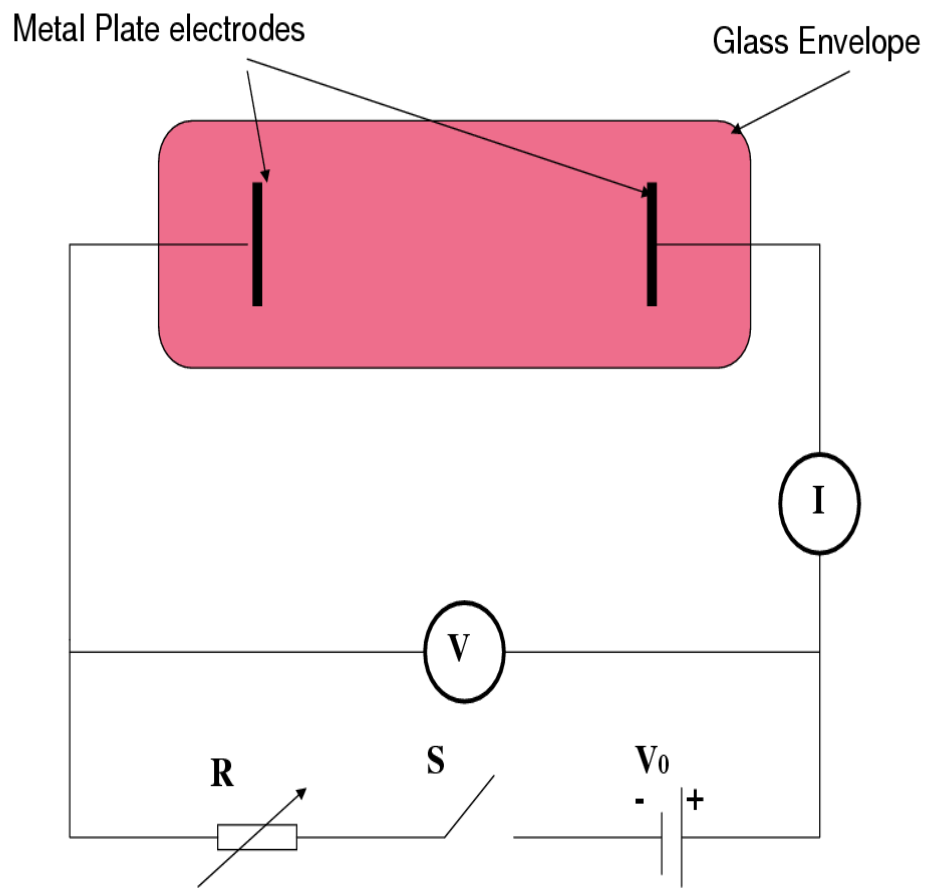


Figure 2.2: Circuit used to establish glow discharge [10].

$$\nabla \vec{E} = \left( \frac{e}{\epsilon_0} \right) (n_i - n_e) = \left( \frac{e}{\epsilon_0} \right) \rho \quad (2.1)$$

where

$e$  = charge of the electron

$\epsilon_0$  = permittivity of the free space

$n_{e,i}$  = charge carrier density, for electron and ions

$\rho$  = space charge density

The so-called electrical characteristic of the discharge is described by the  $I$ - $V$  curve as shown in Fig.(2.3). It is determined by the external parameters  $p$ ,  $d$ , the electrode material, the gas type and the external current density. The desired operating point is fixed by the choice of the external resistor  $R$ .

The electrical characteristic can be subdivided into three region:

1- The low current region,  $I < 10^{-6}$  A; the range of the Townsend discharge; because little or no light is emitted it is also called "dark discharge". The electric field is uniform.

2- With  $I \geq 10^{-6}$  A; the electric field configuration changes due to the onset of space charge distortion. The potential drop  $V_C$  is confined to a short region in front of the cathode (cathode fall). For a certain range of the current the voltage drop  $V_C$  is independent of the current, this is the so called normal glow discharge region. With increasing current  $V_C$  rises; we enter the region of abnormal glow.

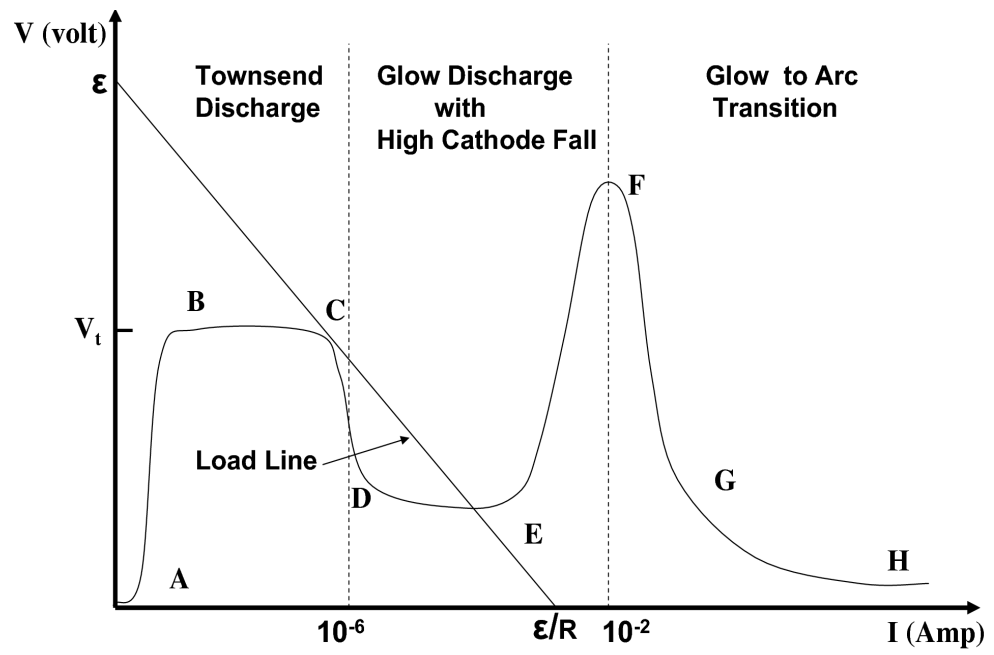


Figure 2.3: Schematic V-I curve of a glow discharge [4].

Large electric fields may occur and, connected with it, the formation of electron beams.

3- Further increase of the current leads to the so-called glow-to-arc transition. The cathode fall undergoes a transformation from cold cathode discharge to a hot cathode discharge with thermionic emission.

In this work, we will be concerned only with region 2 of the plasma characteristic. The plasma parameter ranges which may be expected in a typical glow discharges are:

$10^8 \text{cm}^{-3} \leq n_e \leq 10^{12} \text{cm}^{-3}$ ,  $10^{-4} \text{ torr} \leq p \leq 10 \text{ torr}$ ,  $0.1 \text{ eV} \leq T_e \leq 10 \text{ eV}$ , and  $5 \times 10^{12} \text{cm}^{-3} \leq n_g \leq 3 \times 10^{17} \text{cm}^{-3}$ ; i.e.  $n_e/n_0 \approx 10^{-6} - 10^{-3}$  and  $\lambda_D \approx 10^{-2} - 10^{-1} \text{cm}$ . Where  $n_g$  denotes the density of the neutral atoms,  $T_e$  the electron temperature, and  $\lambda_D$  is the Debye length ( $\lambda_D = 743 (T_e/n_e)^{1/2}$ ) [12, 10].

### 2.3 Positive Column

The *positive column* closes the electric circuit in the space between the cathode layer and the anode. The state of the plasma in a sufficiently long column is completely independent of the situation in the regions adjacent to the electrodes. It is determined by *local* processes and by the electric current. The inevitable loss of charge carriers (electrons) in the column must be compensated for by ionization. The field strength  $E$  necessary for sustaining a stationary plasma is fixed because the ionization rate depends, and quite sharply, on the field,

through the dependence of the electron energy distribution. This determines the longitudinal potential gradient and the voltage difference across a column of a given length. If the spectrum is maxwellian, the relationship can be separated into two causally linked parts:

1-The requirement of the loss compensation by ionization shows what the *electron temperature*  $T_e$  must be.

2-The *field* must supply the necessary energy to the electrons.

The creation and removal of electrons in the column proceed against a steady background of unceasing electron replacement due to the drift motion from the cathode to the anode. It can not be said that a considerable fraction of charge carriers are generated in the glow discharge column. Rather, the majority of electrons reaching the anode enter the column from the outside ( from the cathode region ). The probability for them to be lost on the way is not so high, except for cases of exponentially long inter-electrode separations. The gas temperature  $T_{gas}$  is determined by the balance of the gas energy as a whole. In the positive column of glow discharge, we have  $T_e \gg T_{gas}$  [4].

Since the electron temperature is much higher than that of the positive ions , the insulated walls quickly receive a negative charge and are covered by a positive-ion space-charge sheath. This disturbs the equipotential surface across the tube, which has the effect of moving the cathode nearer to the anode along the glass surface of discharge tube. Equilibrium is quickly established, and the ion and

electron diffusion to the walls is determined by the ambipolar diffusion coefficient. Although the theory of ambipolar diffusion has been investigated extensively, its variation and dependency on the cross-section of the discharge tube has not explained clearly very well until now. Many authors[4, 12, 14] proposed some theories about the construction of the plasma in non-uniform systems, however, their systems were very different from our system, but the theory can be still the same[15, 16]. Hence, under the action of concentration gradients and electric field, the motion of charged particles (ions and electrons) in a gas can be expressed as:

$$\Gamma_e = n_e \bar{v}_e = -D_e \nabla n_e - \mu_e E n_e \quad (2.2)$$

$$\Gamma_+ = n_+ \bar{v}_+ = -D_+ \nabla n_+ + \mu_+ E n_+ \quad (2.3)$$

where  $\Gamma$  represent particle current density;  $n$  is particle density,  $\bar{v}$  is the average drift velocity,  $D$  is the diffusion coefficient,  $\mu$  is the mobility, and  $E$  is the electric field. If the particle densities are sufficiently large, and if only the field present, which is due to the space charge of the particles, then  $(n_+ - n_e \ll n_e)$ , then  $(\Gamma_+ = \Gamma_e)$ . Eqs. (2.2) and (2.3) simplify to:

$$\Gamma = -D_a \nabla n \quad (2.4)$$

where  $\Gamma$  and  $n$  refer to either positive ions or electrons, and  $D_a$  is the ambipolar diffusion coefficient which is given by:

$$D_a = \frac{D_+\mu_- + D_-\mu_+}{\mu_+ + \mu_-} \quad (2.5)$$

where  $D_+$  and  $\mu_+$  are the diffusion and mobility of positive ions respectively, and  $D_-$ , and  $\mu_-$  their are values for negative and/or electrons , respectively [13].

Since  $\mu_e \gg \mu_+$  and  $D_e \gg D_+$ , the quantity  $D_a \approx D_+ + D_e(\mu_e/\mu_+)$  is greater than  $D_+$  but less than  $D_e$ , according to the remark on "speeding-up of the ions" and "restraining" of electrons. For a plasma in equilibrium, where the electron,  $T_e$ , and ion,  $T_i$ , temperatures are equal, the Einstein relations(  $D/\mu = kT/e$  ) yield  $D_a = 2D_+$ . For a non-equilibrium plasma, where the electron temperature is much higher than that of the ions , which is equal to the gas temperature, accordingly;

$$D_a \approx D_e \frac{\mu_+}{\mu_e} = D_+ \frac{T_e}{T_i} = \mu_+ \frac{kT_e}{e} = \frac{2}{3} \mu_+ \bar{\varepsilon}_e [eV] \quad (2.6)$$

where  $\bar{\varepsilon} = 3kT_e/2$  is the mean electron energy [4].

## 2.4 Theory of Positive column

The positive column is a typical plasma having equal concentration of positive ions  $n_+$  and negative ions  $n_-$  and/or electrons  $n_e$ , each with its velocity distribution and characteristic temperature. Following Schottky's theory[17], we assume that there are many electron collisions along the tube radius  $r$ , that is



the electron mean free path  $\lambda_e \gg r$ . Ionization in the gas occurs only by a single collision between the fast electrons and gas molecules. The number of loss is due to ambipolar diffusion, thus both electrons and ions move with the same speed radially outwards. Since they do not recombine in the gas, they neutralize their charges on the wall. Hence their concentration is large at the axis and is practically zero on the insulated wall.

The radial distribution of the electron and ion densities can be described by Schottky diffusion theory. It is well known that at pressures less than a few Torr the positive column spreads laterally to the wall for the large discharge currents. The Schottky theory well describes the spread positive column where the direct ionization balances with the diffusion in the whole plasma. He developed an ambipolar diffusion theory in which he assumed quasi-neutrality of the plasma and neglected the effect of charged particle inertia on the radial structure of the positive column. Many researches show that the radial electron distribution is usually close to the  $J_0$ -Bessel function. In this theory, electrons are in equilibrium with the axial electric field, implying that the energy imported to the electrons by a steady uniform electric field is exactly balanced by energy lost in elastic and inelastic collisions with heavy particles in each volume element of the discharge[18]. The special feature of the electron motion in the potential field of the positive column are related to their acceleration in the longitudinal field, and their deceleration in the radial field. The axial electric field drives the discharge current

$I_d$  and yields the power input to the plasma, which is mainly absorbed by the electron components. However, the radial electric field is caused by the establishment of space-charges and can reach more than  $100\text{ V/cm}$  near the dielectric walls. It accelerates the ions and retards electron movement toward the wall, in such a way that an ambipolar radial flux of electrons and ions is established[19]. At low pressure, electron motion in the radial direction occurs when the total energy is conserved. The electrons at large radii, where the radial electric field is large compared to the axial electric field, are accelerated by the axial electric field to kinetic energy below the ionization potential. At nearly constant energy, they move radially inward, and by ambipolar electrical field they are accelerated above the ionization threshold. After undergoing the elastic ionization collision, the lower-energy electrons moves radially outward.

The current in the positive column is mainly carried by electrons because of the small mobility and drift velocity of the ions. Since an equal number of charges of both signs are produced in the column, more electrons than ions would leave unit length of column, so an accumulation of positive charge will be increased with time. However, because there is a constant influx of electrons from Faraday dark space which constitutes the current. They are removed by the anode at the positive end of the column. There is also a constant flow of positive ions down the column as a result of ionization in the anode region driven into the positive column by the field of the anode.

The elementary theory of the positive column gives a good quantitative description of the relations between the axial and radial electric field, the pressure, the tube radius, and the nature of the gas.

In deriving the particle density equations, the following assumptions were used:

- (i) The Debye length and the electron mean free path are sufficiently smaller than the discharge tube radius.
- (ii) The radial density distributions of the particles are all the same.

This means that the plasma density at the tube wall can be regarded as zero and the ion sheath thickness at the wall can be neglected. Assumption (ii) is valid to the first approximation for both electrons and ions and was often used in the theoretical studies of positive column, when the process of ambipolar diffusion is dominant[20, 21, 22]. Experimental results show that assumption (ii) is also almost valid for the metastable atoms except for the case of (Ne) gas at high pressures[23].

By equating ionization rate and diffusion loss with the assumption that ( $\lambda_e \ll r$ ,  $n_+ = n_e = n$ , and  $(dn_+/dr') = (dn_e/dr') = (dn/dr')$ ), where  $r$  radius of the discharge tube, and  $r'$  any radial position from the axis of the tube, in a along cylindrical positive column a differential equation for charge density can be found directly from Poisson's equation by using cylindrical coordinate with symmetric condition around  $\theta$ , in the form of:

$$\frac{d^2n}{dr'^2} + \frac{1}{r'} \frac{dn}{dr'} + \frac{z}{D_a} n = 0 \quad (2.7)$$

where  $z$  is the number of ionizing collisions per second, and  $D_a$  is the ambipolar diffusion coefficient. Without the term  $zn$  and with boundary condition  $n = 0$  at  $r = R$ , the solution of equation Eq. (2.7) is a Bessel function of zero order:

$$\frac{n_{r'}}{n_0} = J_0 \left( 2.405 \frac{r'}{r} \right) \quad (2.8)$$

where  $n_0$  and  $n_{r'}$  are concentration of the charge at the axis and at a radial distance  $r'$  from the axis (the concentration of charges in a column varies with  $r'$  in a nearly parabolic manner), respectively. In addition, in the condition of equality of ionization frequency and the effective frequency of diffusional loss[17]:

$$\nu_i(E) = \frac{D_a}{\Lambda^2} \equiv \nu_{da}, \Lambda = R/2.4 \quad (2.9)$$

where  $\nu_i n = -D_a \left( \frac{1}{r'} \frac{dn}{dr'} \right)$ .

The case  $zn \ll \nu_{da}$  is realized at low pressure and small transverse dimension ( $\nu_{da} \propto 1/p\Lambda^2$ ), at not too high currents, so that  $n$  is moderate; it is facilitated in monatomic gases where the bulk recombination proceeds slower than in molecular gases.

If  $zn \gg \nu_{da}$ , the recombination of charges in the bulk dominates over their diffusion to the walls. If the diffusion term in Eq. (2.7) is dropped, we find

$\nu_i(E) = zn$ , that is, the density is constant over the cross section. In fact a large gradient of  $n$  appears at the absorbing walls, and the diffusion there cannot be neglected. Electron or ion density changes only slightly near the center of the discharge tube but drops sharply near the walls [4].

The voltage gradient  $E$  in the positive column is given by balancing the energy that the electrons gain from the electric field per second and the energy they lose by collisions, elastic collision  $L_{eL}$  and inelastic collision  $L_i$ , per sec. Therefore:

$$eE\vartheta_d = L_{eL} + L_i \quad (2.10)$$

where

$$L_{eL} = P \int_0^\infty G_{eL} \frac{m\vartheta^2}{2} \frac{\vartheta}{e} f(\vartheta) d\vartheta \quad (2.11)$$

$$L_i = P \int_0^\infty eV_e \eta \frac{\vartheta}{e} f(\vartheta) \quad (2.12)$$

where  $f(\vartheta)$  is the velocity distribution function,  $\lambda_e$  mean free path of electron,  $\eta$  ionization and excitation function,  $V_e$  critical potential,  $\vartheta$  drift velocity,  $G_{eL}$  the energy lost in elastic collision,  $e$  and  $m$  are electron charge and mass, respectively;  $P$  the pressure, and  $T_e$  the electron temperature. Assuming the electron mean free path to be independent of energy, we have ( $T_e \propto E/P$ ), if collision frequency is assumed to be constant, we have ( $T_e \propto (E/P)^2$ ). It was shown that except at very low pressures, the electron drift velocity is much lower than the random

one, under the conditions exactly corresponding to the glow discharge positive column. Roughly speaking, the electron spectrum is said to be maxwellian if the frequency of the electron-electron collisions is appreciably higher than the energy loss frequency[4, 12]. From the equation of ambipolar flow,

$$\vartheta_a = -\frac{D_+}{n} \frac{dn}{dr} + \mu_+ E = -\frac{D_e}{n} \frac{dn}{dr} - \mu_e E, \quad (2.13)$$

the radial field:

$$E_r = \frac{1}{n} \frac{dn}{dr} \frac{D_+ - D_e}{\mu_+ + \mu_e} \approx \frac{1}{n} \frac{dn}{dr} \frac{D_e}{\mu_e} \approx \frac{1}{n} \frac{dn}{dr} \frac{kT_e}{e} \quad (2.14)$$

and then the potential can be found as:

$$-V_r = \frac{kT_e}{e} \ln \frac{n_0}{n_{r'}} \quad (2.15)$$

or

$$\frac{n_{r'}}{n_0} = \exp - \left( \frac{eV_r}{kT_e} \right) \quad (2.16)$$

Showing that the concentrations of charges follow Boltzmmann distribution[12].

## CHAPTER 3

### ELECTRICAL LANGMUIR PROBE

#### 3.1 Overview of Langmuir Probes

Electrostatic plasma probes were invented by the scientist Irving Langmuir in the year 1924. His relatively simple devices were the first plasma diagnostic instruments and still bear his name, as electrostatic probes are most commonly referred to as "Langmuir probes". They are capable of measuring electron density, ion density, electron temperature, plasma potential and floating potential. Their accuracy in measuring these plasma properties depends on the particular situation in which they are used. Their use is limited to cool plasmas which will not melt or rapidly erode their surfaces because they are material probes that must be inserted into the plasma. Despite their simple construction and operation, the interpretation of their data can be quite complex[24].

From an experimental point of view the Langmuir probe is simply a current collector surface placed into the plasma environment. Probes of many types were developed and used with success in the case of practical applications. Such as emissive probes, double probes, capacitive probes, oscillation probes, probes in

flowing or high pressure plasmas, and probes in a magnetic field. Our measurements were carried out using cylindrically shape double probes with 0.175 mm base diameter and 0.5 mm height, made of tungsten wire. The wire must be well insulated to avoid take-current collection. Because the Langmuir probe gives local plasma information it must be movable to reach any desired point of plasma (radially) chamber's volume.

The probe technique is an important one because it has an advantage over all diagnostic techniques: it can make local measurements. Almost all other techniques, such as spectroscopy or microwave propagation, give information averaged over a large volume of plasma [3].

### 3.2 Probe Theory

Langmuir probes generally consist of one or more metallic, conducting electrodes inserted into a plasma. The "simple" Langmuir probe is a single electrode where one conductor is inserted into the plasma.

The probe is a conducting wire typically made out of a high temperature metal such as tungsten or nickel, and is surrounded by an insulating sleeve, usually made out of a ceramic such as alumina. The conductor extends out of the insulator some distance to form the probe area.

The theory of the flow of charge carriers to an electrical probe can be extremely complex. The numerous analysis presented arises from the need to apply the



electrical probe method to such a wide range of plasma.

A simplified introduction to the electrical probe method, as applied to this type of gas discharge, will be given here. The following assumptions are made:

- 1- Electron and ion concentrations are equal.
- 2- Electron and ion mean free paths are much larger than the probe radius.
- 3- Probe radius is much larger than the Debye length.
- 4- There is a Maxwellian distribution of electron and positive ion velocities.
- 5- Electron temperature ( $T_e$ ) is much larger than the positive ion temperature ( $T_i$ ) or ( $T_{gas}$ ).

A low pressure plasma is defined as one in which a probe of sufficiently small diameter produces a negligible disturbance to the carrier concentration and in which the great majority of the applied probe to plasma potential is developed across a region that is much thinner than the carrier mean free path[25].

In the low density regime, it is a common practice in the industry to use the Orbital Motion Limited (OML) theory of ion collection. This theory can be applied successfully well outside its intended range, but its error is greatly enhanced at higher density. For probe radii much smaller than  $\lambda_D$  (thick sheath), and if the potential around the probe decreases more slowly than  $r^{-2}$ , we are in the Orbital Motion Limit (OML) regime[26]. In this regime, for every ion energy there exists an ion impact parameter that makes the ion hit the probe with a grazing, or tangential, incidence. The maximum impact parameter for hitting the

probe is the simple function of the ion initial energy and of the probe potential with respect to the plasma. When  $(r_p/\lambda_D)$  increases the OML may break down, where  $r_p$  is the probe radius and  $\lambda_D$  is Debye length ( $\lambda_D = 743(T_{eV}/n_e)^{1/2}$ ). Since the diameter of our probes ( 0.175 mm) less than 0.2 mm the OML can be used[27, 28].

### 3.3 Electrical Probe at Low Pressure Discharge

#### 3.3.1 Single Probe

Probes may have a planar, spherical, and cylindrical shapes. The latter are applied most often in practice because, firstly, there is a definitive theory describing the behavior of the sheath around the probe, and thus, the ion current expansion. This allows the measurement of  $n_+$  at highly negative voltages and the calculation of the fast electron current to the probe. Secondly, it is possible to use small area probes and thus reduce the effects due to depletion of low-energy electrons.

Although single Langmuir probe measurement of electron temperature is in general straightforward, the measurement of plasma density is more difficult and contains larger experimental errors. Since the current below the plasma potential has an exponential dependence on voltage, a small error in the estimation of the plasma potential can result in a large error in the density measurement. The current collected at the plasma potential is also strongly influenced by probe

cleanliness apparently because the low energy electrons are reflected. Finally, using the electron saturation current to measure the electron density is difficult because analytical solutions for the functional dependence on the voltage is only possible for the limits  $r_p/\lambda_D \ll 1$  or  $r_p/\lambda_D \gg 1$  which are often not easily obtainable, where  $r_p$  is the probe radius and  $\lambda_D$  is Debye length[29, 30]. Therefore the fast computerized three couples of double probe system (TCDP) has been developed and used in our system.

### 3.3.2 Double Probe

When two electrodes are used, referred to as a "double" Langmuir probe, they are inserted into the plasma near each other so that they sample the same plasma properties. Both electrodes are initially floating at potentials below the plasma potential. A power supply is connected between the two electrodes so that a potential difference can be applied between the two electrodes. The potential difference is varied using the power supply, while the current between the probes is recorded. The main advantage of using a double Langmuir probe instead of a simple Langmuir probe is that there is only a very small net current drawn from the surrounding plasma, keeping plasma disturbances to a minimum. The current to the double Langmuir probe is constrained by the fact that the current collected in one electrode must be taken from the other electrode. Thus one end of the system is always limited in drawing the ion saturation current at maximum,

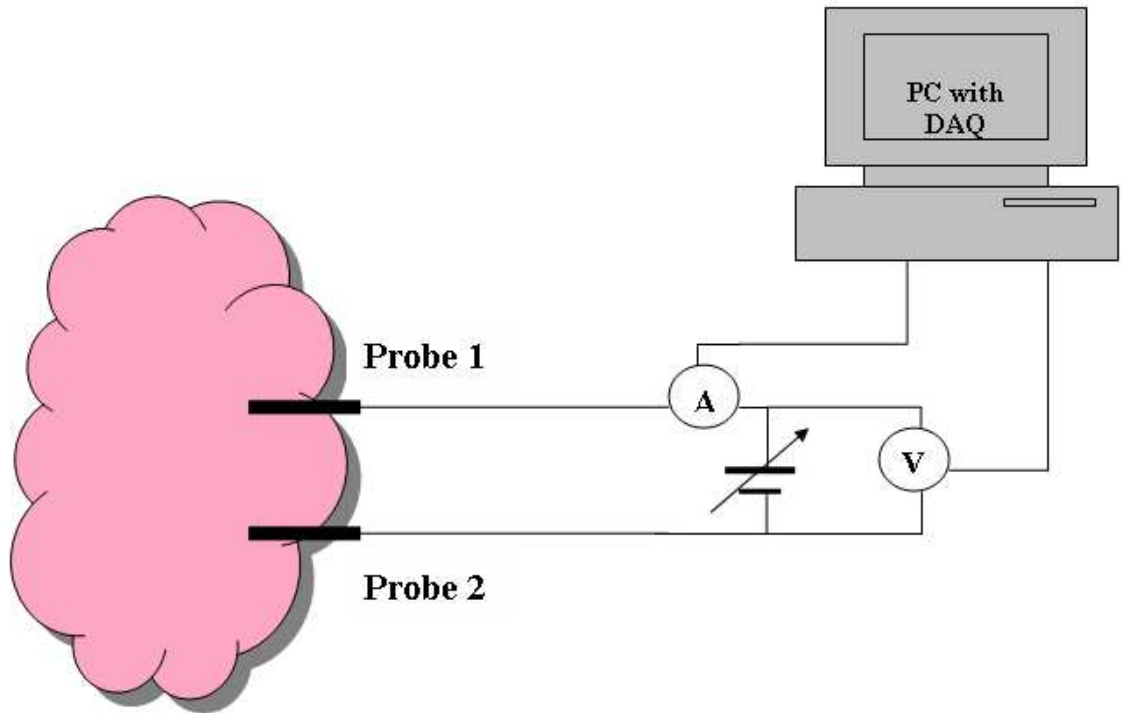


Figure 3.1: Electrical circuit for double probe measurement.

which tends to be a very small current. It can be used for determining the electron temperature and the plasma density (from the ion saturation current).

The double probes has been studied, both theoretically and experimentally, under various conditions by Johnson and Malter (1950), Cozens and Von Engel (1965), and Bardley and Mathews (1967)[31, 32, 33] and several researchers as a tool for measurement of plasma characteristics.

The double probe method (DP) make use of two probes, each similar to the single probe (SP). They are interconnected as shown in Fig.(3.1).

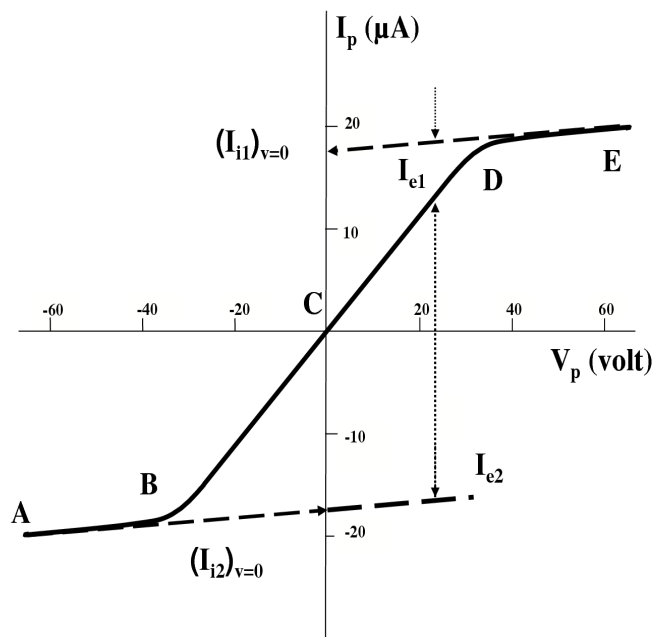


Figure 3.2: Characteristic of symmetric double probe.

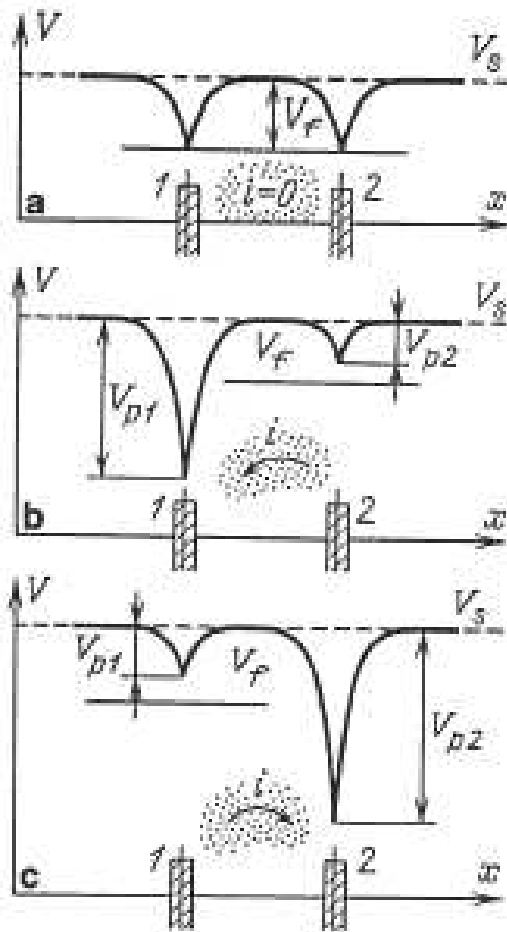


Figure 3.3: Double probe potential:(a)Floating potential, no current through the probes; (b) Left-hand probe is strongly negative, and receives ionic saturation current.(c) Polarity reversal; the right-hand probe is strongly negative[4].

As in the (SP), the (DP) is based on the Boltzmann relation and the plasma sheath properties of a gas discharge, and the electron temperature will be determined by the way in which  $I_d$  (discharge current) varies with  $V_P$  (probe voltage). In this case, the probe current will be smaller than the discharge current. In addition, (DP) is based on an application of Kirchhoff's-current law which requires in this case that at any instant the total net current of positive ions and electrons flowing to the system from the plasma must be zero.

An idealized plot of the measured current as a function of the potential difference, as the latter changes from a fairly large value in one direction to a similar value in the opposite direction, is shown in Fig.(3.2). For simplicity it is assumed that the two probes are identical for our case, so that the two portions of the curve have the same shape.

Suppose the voltage applied from the battery is such as to make probe2, highly negative with respect to probe1. Probe2 will then collect positive ions at the maximum rate, so that the observed current is equal to  $I_{i2}$ , the random ion current to probe2. Probe1 will then collect an equivalent number of electrons, but no ions. However, since the ions are more slowly collected than the electrons, the maximum ion current can be measured, rather the maximum possible electron current, which determines the maximum (absolute) value of the current flowing through the plasma between the probes.

As the potential of probe2 is made less negative Fig.(3.2), the current remains

constant along  $AB$ , but in the vicinity of  $B$  the potentials are such that some electrons, in addition to positive ions, are collected at probe2. The absolute magnitude of the net plasma current  $I_P$  thus decreases  $B$  to  $C$ . At  $C$ , the external voltage between the probes is zero; both probes then have the same potential with respect to the plasma and no current flows Fig.(3.3)a. As the direction of the applied voltage is changed, the probe1 now becomes negative with respect to probe2 Fig.(3.3)b, the situation is exactly reversed, and the curve  $CDE$  in Fig.(3.2) is obtained for the current  $I_P$ , which now flows in the opposite direction Fig.(3.3)c, as a function of the voltage  $V_P$  applied between the probes. Thus,  $DE$  gives  $I_{i1}$ , the random ion current to probe1, and this will be the same as  $I_{i2}$  if the probes are identical.

The total current to the system can never be greater than the saturation ion current, since any electron current to the total system must always be balanced by an equal ion current. Thus the disturbance on the discharge is minimized. This has the disadvantage, however, that only the fast electrons in the tail of the distribution can never be collected; the bulk of the electron distribution is not sampled.

The condition that the system be floating is:

$$I_{i1} + I_{i2} - I_{e1} - I_{e2} = 0 \quad (3.1)$$



The current  $I_P$  in the loop is given by

$$I_{i1} + I_{i2} - (I_{e1} + I_{e2}) = 2I_P \quad (3.2)$$

If we add and subtract Eq. (3.1), and Eq. (3.2), we obtain:

$$I_P = I_{e1} - I_{i1} = I_{i2} - I_{e2} \quad (3.3)$$

The current  $I_e$  are given by

$$I_e = \frac{1}{4} neA\bar{v}_e \exp\left(-\frac{eV_f}{kT_e}\right) = neA \left(\frac{kT_e}{2\pi m}\right)^{1/2} \exp\left(-\frac{eV_f}{kT_e}\right) \quad (3.4)$$

where  $n$  is the electron density,  $A$  is the probe area,  $\bar{v}_e$  is the average electron velocity,  $V_f$  is the floating potential, and  $T_e$  is the electron temperature in  $K^0$ .

For the electron current density to a probe in the transition region:

$$I_{e1} = A_1 j_{re1} \exp\left(-\frac{eV_1}{kT_e}\right) \quad (3.5)$$

and

$$I_{e2} = A_2 j_{re2} \exp\left(-\frac{eV_2}{kT_e}\right) \quad (3.6)$$

Here  $I_{re} = Aj_{re}$  is random the electron current, and  $j_{re}$  is the random electron current density. Substituting this into the first of Eq. (3.3) and using ( $V = V_1 - V_2 > 0$ ), we have:

$$I_P + I_{i1} = A_1 j_{re1} \exp\left(-\frac{eV_1}{kT_e}\right) = A_1 j_{re1} \exp\left(-\frac{e(V + V_2)}{kT_e}\right) = \frac{A_1}{A_2} I_{e2} \exp\left(-\frac{eV}{kT_e}\right) \quad (3.7)$$

From the second of Eq. (3.3),

$$\frac{I_P + I_{i1}}{I_{i2} - I_P} = \frac{A_1}{A_2} \exp\left(-\frac{eV}{kT_e}\right) \quad (3.8)$$

The basic assumption of this theory is that the probes are always negative enough to be collecting essentially saturation ion current; therefore,  $I_i$  can be accurately estimated at any  $V$  by a smoothly extrapolating the saturation portion of the double-probe characteristic.

Since we have probes with equal area ( $A_1 = A_2$ ) then  $I_i \cong I_{i1} \cong I_{i2}$ , the formula:

$$I_P = I_i \tanh\left(\frac{V}{2T_{eV}}\right) + \frac{V}{R} + I_0 \quad (3.9)$$

has been used [3, 34] to fit the experimental curve accurately for all of (TCDP). Where  $R$  accounts for the effects of sheath expansion on probe current ( $I_i$ ) as well as leakage current between the electrodes (due to the possible contamination), and  $I_0$  account for any displacement current due to a time varying floating potential and the difference in stray capacitance to ground for each electrode. Electron temperature can be determined directly from the fit parameters.

However, our small correction to fit this formula to the  $I - V$  characteristics, which are shifted from the original point, is that:

$$I = I_p \tanh\left(\frac{(V - V_0)}{2T_{eV}}\right) + \frac{(V - V_0)}{R} + I_0 \quad (3.10)$$

where  $V_0$  is any constant, which can be fixed after getting a good result, then start the fit method "Levenberg -Marquardt algorithm" from the beginning. Therefore, the electron temperature can be determined directly from the fit parameters[35].

The electron density  $n_e \approx n_i$  (assuming quasi-neutrality, and usually equal to the plasma density  $n$ ), is obtained from the formula :

$$I_p = Ane^{3/2} \left(\frac{T_{eV}}{M_i}\right)^{1/2} \quad (3.11)$$

where  $T_{eV}$  is the electron temperature in eV,  $e$  is the electron charge,  $A$  is the probe tip area, and  $M_i$  is the ion mass. The assumptions involved in the application of Eq. (3.2) are that the electron velocities are isotropic and Maxwellian, and that the sheath is collisionless. As the ratio  $(r_p/\lambda_D)$  increases, Eq. (3.11) is no longer applicable [27, 36].

A Langmuir probe immersed in a plasma will, under equilibrium conditions, assume a negative potential (the floating potential) with respect to the plasma, so that the random electron current density at the probe surface is attenuated from its bulk plasma value to a quantity equal to the random ion current density.

Then the floating potential  $V_f$  is defined by  $I_p = -I_e$ . Then by setting Eq. (3.4, and 3.11) equal yields:

$$V_f = -\frac{T_{eV}}{2} \ln \left( \frac{2M_i}{\pi m_e} \right) \quad (3.12)$$

Since  $V_f \approx 5T_{eV}$ , the sheath is well established at this potential, and the expected  $I_i(V_f)$  can be calculated without the uncertainties inherent in extrapolation to the space potential  $V_s(= 0)$  due to the weak ion accelerating field there[37].

## CHAPTER 4

### EXPERIMENTAL APPARATUS

#### 4.1 Discharge Tube and Double Probe System

Fig.( 4.1) is the schematic diagram of the apparatus used as a discharge reactor system which is made of pyrex glass. Since, discharge tube with a variable diameters in the same system of glow discharge has not studied very well until now. The outer glass is (uniform cylindrical) of length (30 cm) with inner diameter(5.6 cm), and the internal one is (nonuniform) fixed to the external glass. It is constructed in a way that the diameter has been changed from the cathode to the anode but with symmetry in the middle point. The diameters for regions near electrodes are (4.2 cm), but in the middle is (2.8 cm). Argon has been used as a discharge gas, since it has the advantage of a relatively complete set cross section and a minimum of discharge chemistry.

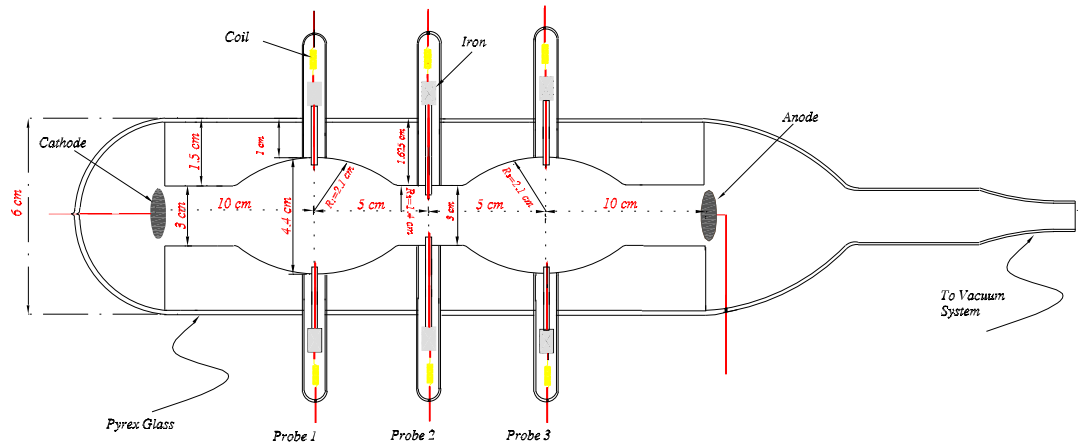


Figure 4.1: Schematic diagram of experimental apparatus.

Because of high melting point as well as low sputtering yield, the cylindrical type of tungsten wire has been used as a probe, and coated with capillary Pyrex tube. The tips of cylindrical double probes are equal in length (0.5 mm) with radius ( $r_p = 0.0875$  mm).

An external adjustment method (magnetic effect on a cylindrical iron placed at the probe ports) has been used to change the radial position of the probes. The iron cylinder is covered with a glass tubing to avoid any chance of contamination in cell atmosphere. The moveable (TCDP) were inserted into the plasma through the orifice in the tube wall perpendicularly to the discharge axis, and they were fixed near the axis of internal discharge tube. The distance between each couple of probes is 5 cm in the axial direction.

Using one side of the each double probe as a fixed probe at the center and moving the other probe, the measurements of the radial potential gradient has been done at constant pressure (0.7 torr). Since, the distance between each couple of probe will not be very large (1.9 cm for probe 1 and 3, and 1.2 cm for probe 3) such that the plasma parameters could not different, where the probes are located.

A computer-controlled data acquisition (from National Instrument) has been employed for this work. The system consists of a compatible PC hosting a DAQ card(NI 6014, 16 bit and 200KS/s). The input voltage will be controlled by (DAC) (digital-to-analog converter), by generating the square wave. Therefore, the current from each probe is recorded for each voltage step at a sampling rate of up to 75 Hz [38]. The National Instrument (SC-2345) Series which is the enclosure for SCC signal conditioning modules connect directly to 68-pin ADQ device. The SCC-AO10 is an isolated voltage output module with an output range of  $\pm 10$  V. The output voltage level is controlled by the DAC output of an E Series ADQ device using LabVIEW programme. This  $\pm 10$  V will be amplified to a  $\pm 75$  V output with PA85 (high voltage operational amplifier) to the probe.

The currents flowing in the probe circuit (there are three separate circuits) Fig.( 4.2) can be detected using the (AD620) from Analog Device. It is a low cost, high accuracy instrumentation amplifier that requires only one external resistance to set gains( programmable gain with bandwidth 120 kHz at  $G =$

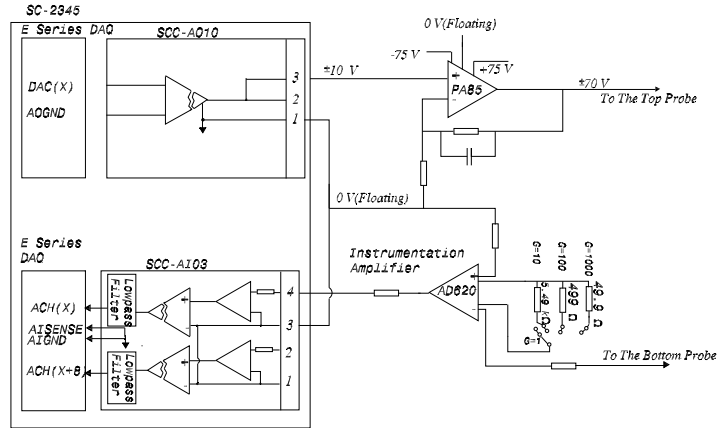


Figure 4.2: Schematic diagram of the double probe diagnostic system.

100) of 1 to 1000. Hence, the probe circuit has been developed, and can be used for magnetized plasma or slowly oscillating systems. In addition, the SCC-AI Series isolated analog input modules (SCC-AI03 with input impedance 100 M $\Omega$ ) can extract a relatively low-amplitude input signal from a high-common-mode voltage, so the E Series DAQ device can measure the input signals. It can also amplify and filter the input signal (with bandwidth 10 kHz), resulting in higher measurement resolution and accuracy. The inputs are designed in a floating (non-referenced) single-ended configuration. LabVIEW Express program has been used to control the whole system, and the three regions have been checked simultaneously in a very short time, approximately 0.5 ms for each probe.



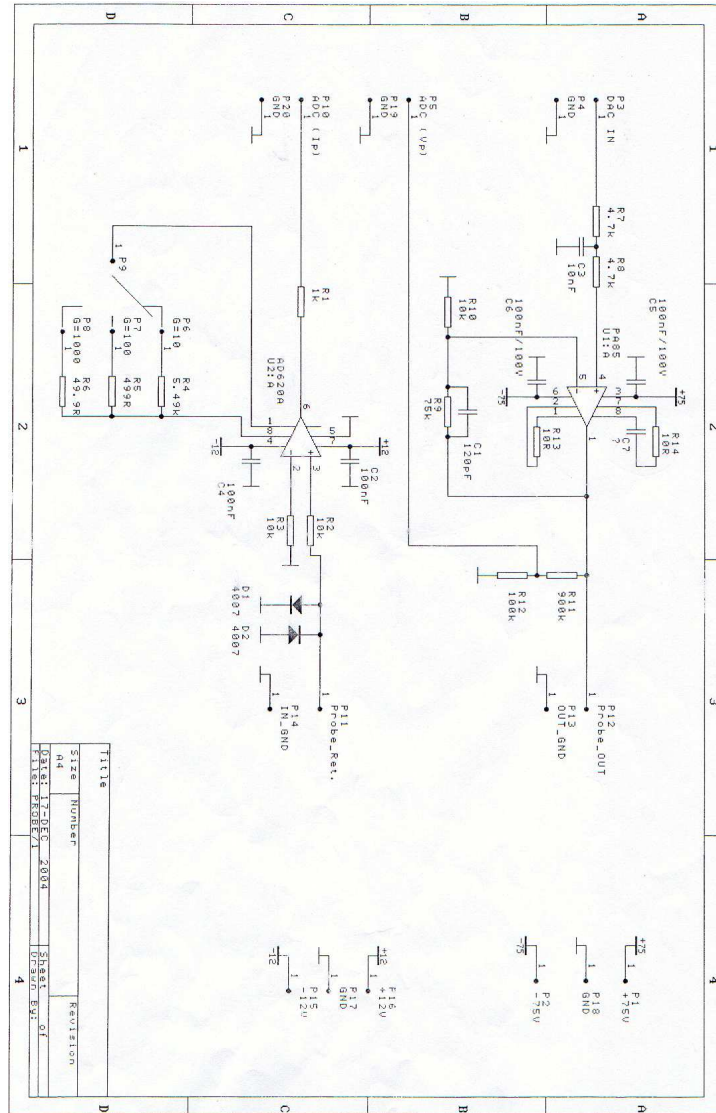


Figure 4.3: Floating Langmuir probe derive and current amplifier.

PROBE Top Overlay

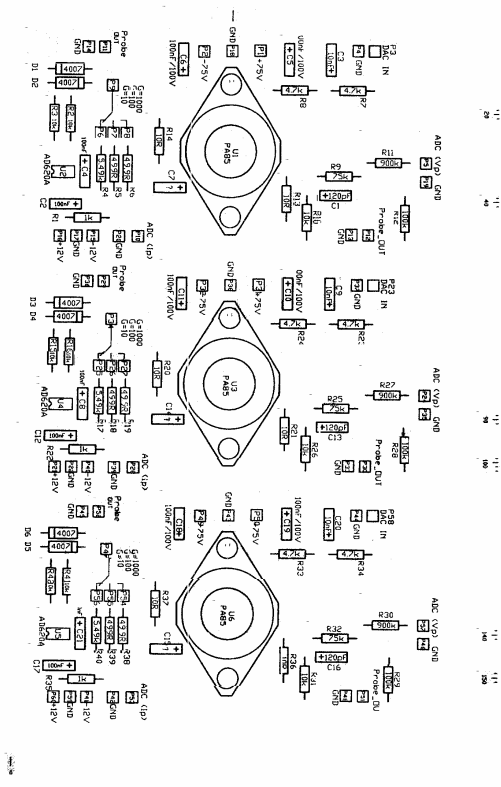


Figure 4.4: Floating Langmuir probe derive and current amplifier.

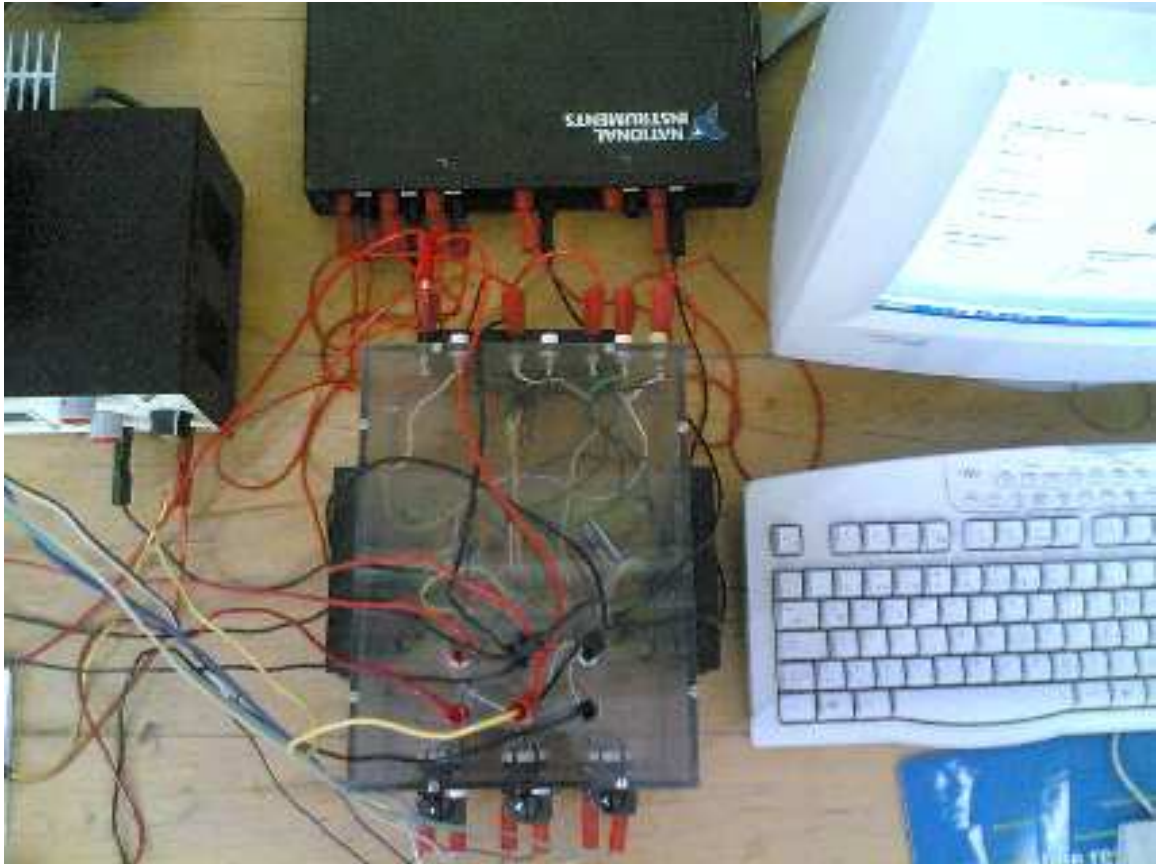


Figure 4.5: The electronic parts of the isolated computer controlled three couples of double probe (TCDP) system.

## 4.2 The Pressure Measurement System

The experiments are performed using two-stage vacuum pump (mechanical and oil diffusion) to evacuate the whole system down to  $10^{-4}$  torr. The chamber pressure was controlled with wide range gauge an *MKS* SensaVac Series 953 Pirani/Cold Cathode Ionization Vacuum Gauge (from  $10^{-9}$  torr to atmosphere). An analog-to- digital converter has been used as a digital gauge pressure with an input voltage (0-4 volt) for Pirani (for range until  $10^{-4}$  torr) or (0-7 volt) for the cold cathode (for range  $10^{-2}$  to  $10^{-9}$  torr).

## CHAPTER 5

### RESULTS AND DISCUSSION

#### 5.1 Double Probe Characteristics at Different Pressures and Constant Distance from The Axis:

##### 5.1.1 Current-Voltage Characteristics:

A series of ( $I - V$ ) measurements, as shown in Figs.( 5.1 and 5.2), only to show the effect of the low and high discharge currents, have been carried out to investigate the behavior of electric discharge in the tube over a certain range of argon gas pressures and discharge currents for all three double probes at the same time. All measurements have been done at discharge currents ( $I_d = 5$  mA, 10 mA, and 15 mA), and pressure ranges ( $p = 0.3 - 2.1$  torr), when the probes 1, 3, and 2 are fixed radially at the distance 1.7 cm, and 1 cm from the wall of the inner tube, respectively.

It is clear that as the pressure increases the characteristic curve will shift toward the negative direction. That can be attributed to the fact that the longitudinal voltage gradient increases with pressure at fixed discharge current and decreases as the discharge current increases because of the increase in the molecular

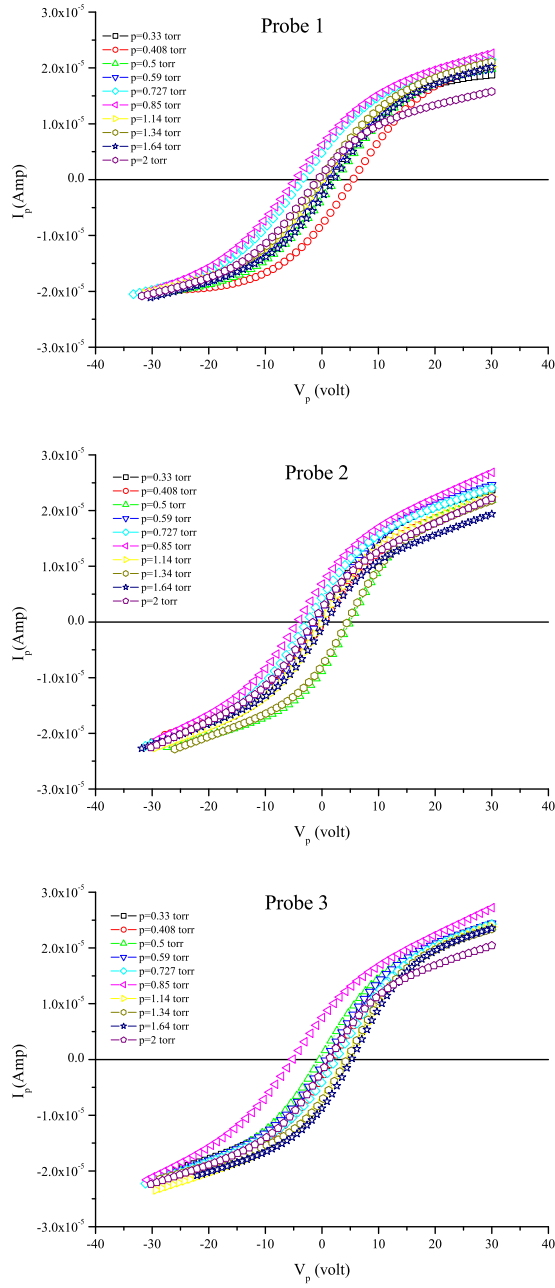


Figure 5.1: Double probe characteristic in argon gas at  $I_d = 5$  mA (at fixed radial distance (1.7 cm), and (1 cm) for probes 1, 3 and 2 respectively), and different pressures.

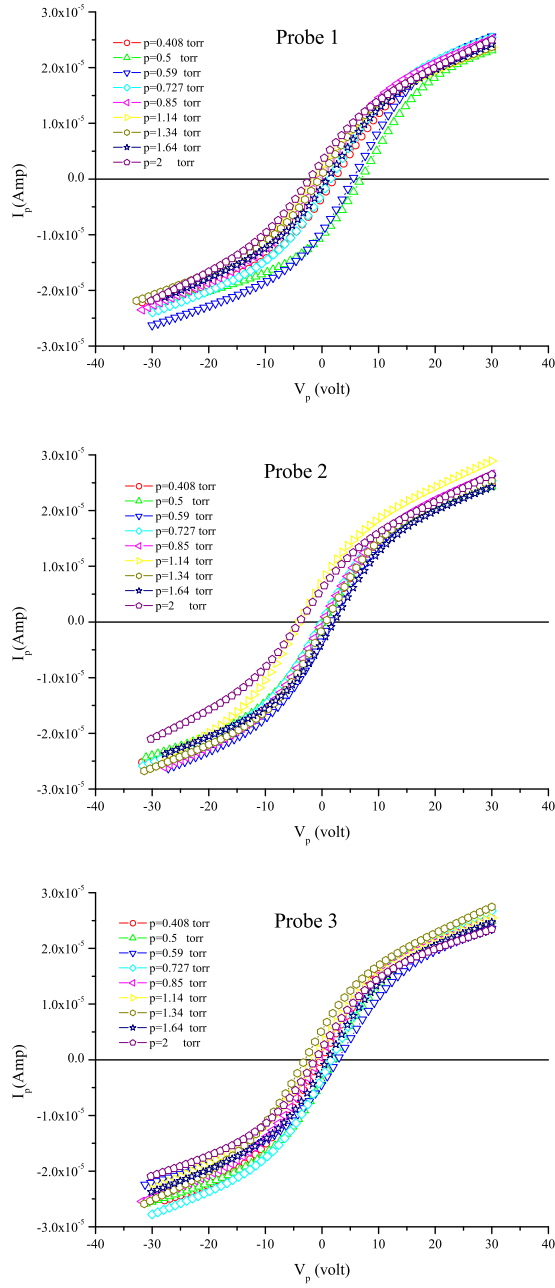


Figure 5.2: Double probe characteristic in argon gas at  $I_d = 15$  mA (at fixed radial distance (1.7 cm), and (1 cm) for probes 1, 3 and 2 respectively), and different pressures.

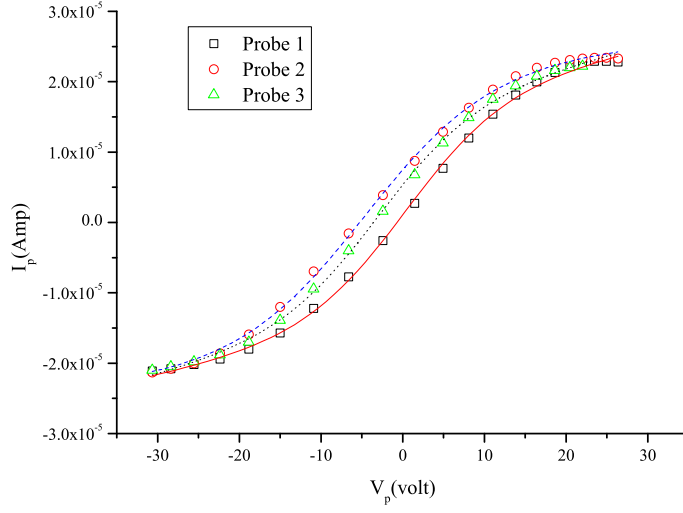


Figure 5.3: The experimental (symbols) and theoretical (lines) I-V curves for probes (P1-continuous, P2-dash, and P3- dots, for all figures) at discharge current  $I_d=10$  mA and pressure 0.33 torr at fixed radial distance (1.7 cm), and (1 cm) for probes 1, 3 and 2 respectively.

ion population with pressure. However, this molecular ion population decreases with the current[39].

### 5.1.2 The Electron Temperature and Density

The variation of the electron temperature  $T_e$ , electron density  $n_e$ , and axial electric field  $E$  in argon gas for different values of the discharge current  $I_d$  as a function of  $(pR)$ ;  $p$  is the gas pressure in torr, and  $R$  is the tube radius ( $R_1$  and  $R_3$  are equal to 2.1 cm, and  $R_2$  is 1.4 cm) are shown in Figs.( 5.4 and 5.5).

The common trends of the curves are that the electron temperature (electron



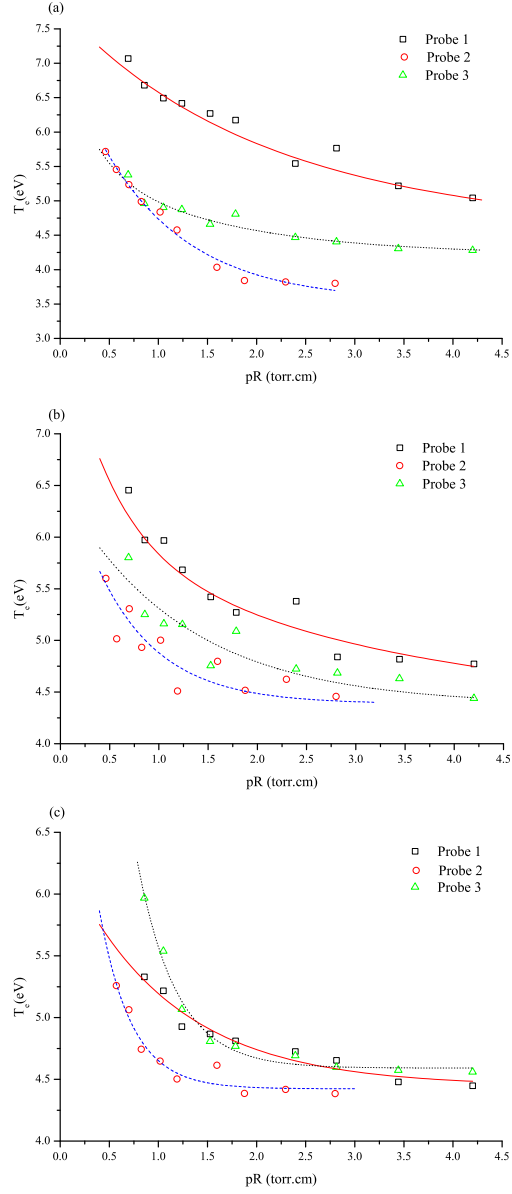


Figure 5.4: Electron temperature as a function of  $pR$  at discharge current (a)  $I_d = 5$  mA, (b)  $I_d = 10$  mA, and (c)  $I_d = 15$  mA, at fixed radial distance (1.7 cm), and (1 cm) for probes 1, 3 and 2 respectively.

density) for all regions tends to increase (decrease) steeply as the product  $pR$  decreases (increases), except at the probe 3 the electron temperature increases sharply, at discharge current  $I_d = 15$  mA, with  $pR$ . Since, as the pressure increases the mean free path and the energy acquired by the electrons decreases, and this leads to reduce of the ionization process.[40, 41, 42, 43].

On the other hand, the electron temperature and densities remain approximately constant with discharge current at probes 2 and 3. However, the  $T_{e1}$  decreases and  $n_{e1}$  increases with  $I_d$  at probe 1. These are due to the collision loss factor is increased with increasing of the discharge current because the cumulative ionization effect brings the increase of the inelastic collision loss by electrons with lower energy as shown by Dote and Kaneda[44]. In addition, at low current densities, the diffusion coefficient is greater than the ambipolar value necessitating a higher ionization rate and higher electron temperatures [45].

If we take all these results under consideration, our system has big differences from other uniform dc glow discharge systems. Since, as can be seen from results, the electron temperature and density have unexpected behavior at different radii of the same discharge tube. For example, for the traditional dc plasma,  $T_{e2}$  must be approximately equal to  $T_{e3}$ , and  $n_{e3}$  must be greater than  $n_{e2}$  and so on. The reasons behind these are that the decrease of the discharge tube radius gives rise to the growth of the energy loss and de-excitation of excited argon atoms on tube walls[4, 46, 15, 16].

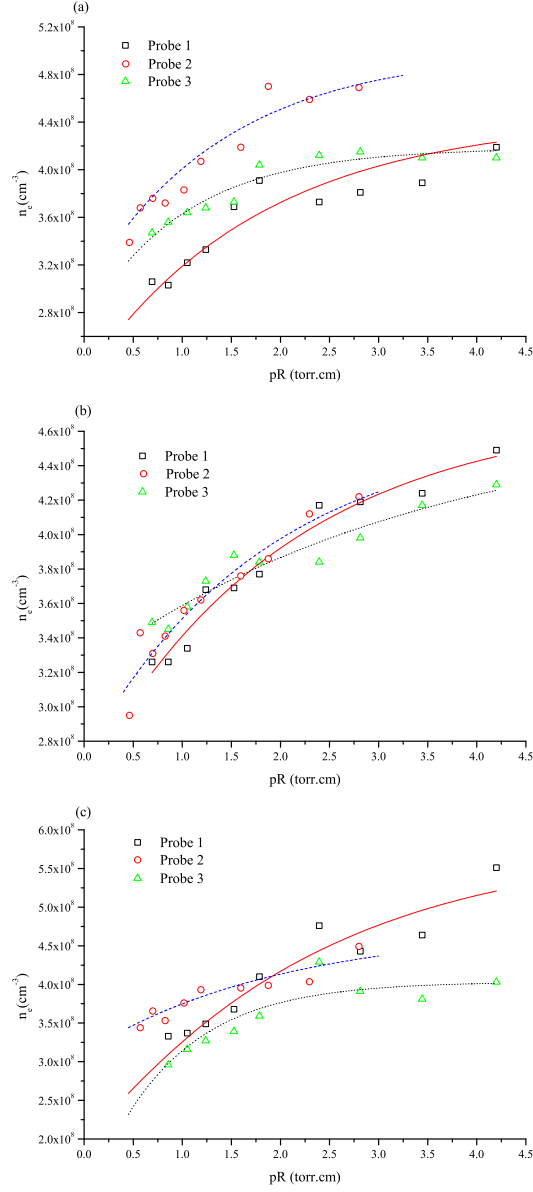


Figure 5.5: Electron density as a function of  $pR$  at discharge current (a)  $I_d = 5$  mA, (b)  $I_d = 10$  mA, and (c)  $I_d = 15$  mA, at fixed radial distance (1.7 cm), and (1 cm) for probes 1, 3 and 2 respectively.

Because the electron density is calculated from the ion saturation current (Eq. 3.11), and electron temperature calculation, error in estimating the ion saturation current or the electron temperature are compounded in the calculation of the electron density. Typical estimates for the errors in electron temperature and electron density are (10-20)% and (25-50)% respectively [47, 48].

### 5.1.3 The Electric Field

Another important parameters, for the description of the positive column behavior is the axial electric field  $E$ . As can be seen from Fig.( 5.6),the electric field, in general, decreases with  $pR$  and more less with discharge current  $I_d$ . Since, as the electron temperature increases with decreasing the pressure according to the ambipolar diffusion theory by Schottky [17],  $E$  tends to increase as  $pR$  decrease. The dependence of  $E$  on  $pR$  is due to the diffusion loss to the wall. In addition, some decrease in electric field as the discharge current increases is caused by a rise in gas temperature. The reduced electric field at small radius is coming from the relation between  $T_e$ ,  $E$ , and  $n_e$ . In the case of longitudinal inhomogeneities the field and electron temperature are reduced at points of high electron density, and vice versa. Although the  $E$  has been changed in all regions, at low discharge current, but this change has disappeared at high discharge current for the same radii, as Fig.( 5.6c)[49].

On the other hand, the density of meta-stable gas atoms depends on the

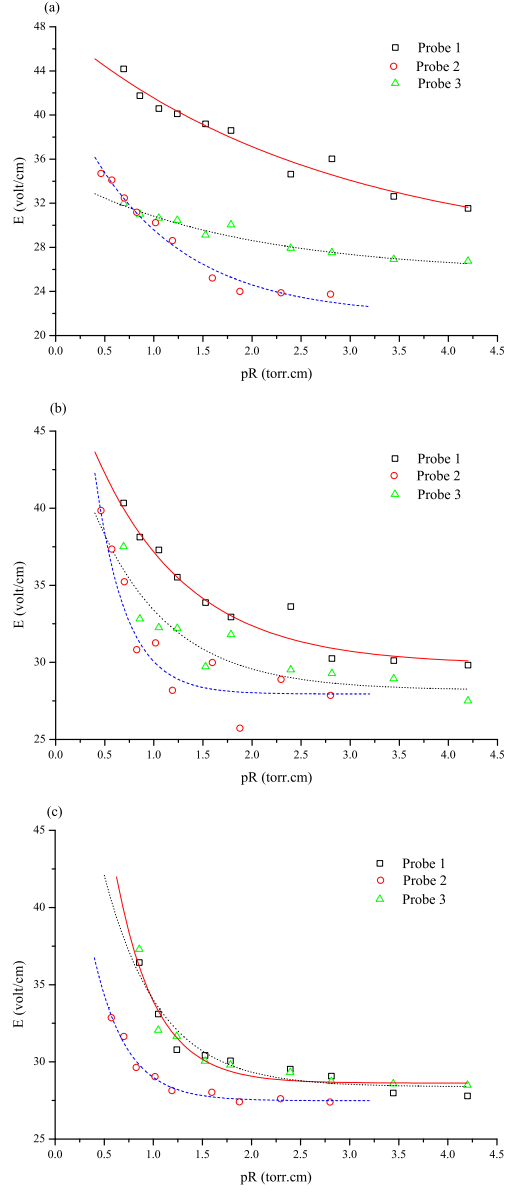


Figure 5.6: Axial electric field as a function of  $pR$  at discharge current (a)  $I_d = 5$  mA, (b)  $I_d = 10$  mA, and (c)  $I_d = 15$  mA, at fixed radial distance (1.7 cm), and (1 cm) for probes 1, 3 and 2 respectively.

electron density which is usually proportional to  $I_d$ . As the meta-stable gas atom can be ionized by low energy electrons, the increases of its density causes the lowering of  $T_e$  related to  $E$ . The gas heating can give rise to a decreasing voltage drop along the positive column, and hence a decrease in the axial electric field  $E$  with increasing current[39] as can be seen from Fig.( 5.7).

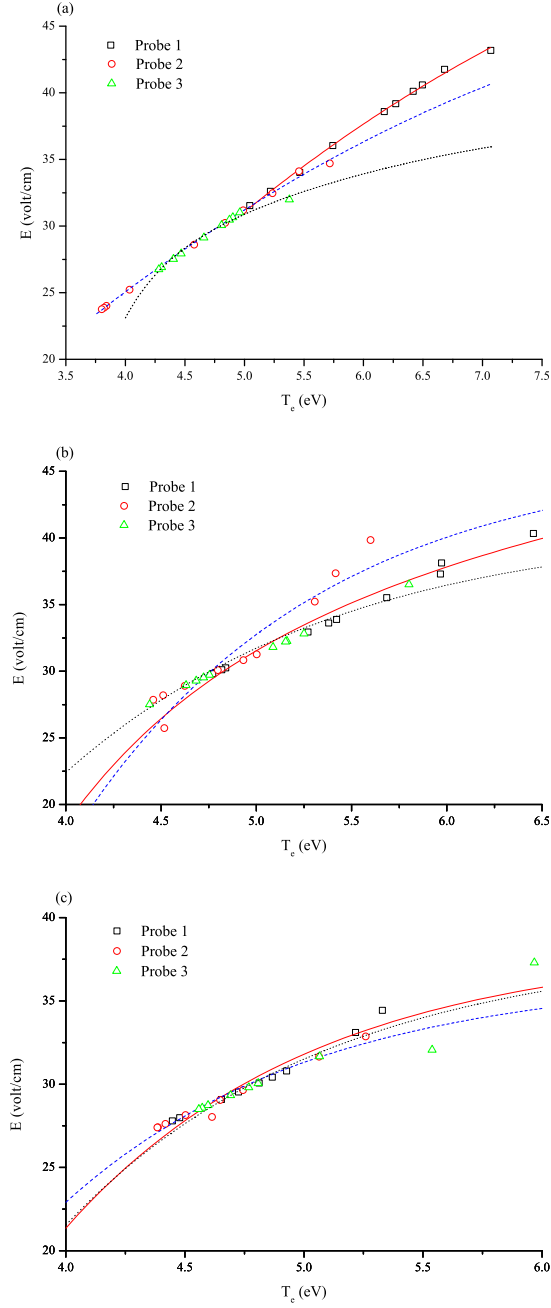


Figure 5.7: Electron temperature as a function of the axial electric field at discharge current (a)  $I_d = 5$  mA, (b)  $I_d = 10$  mA, and (c)  $I_d = 15$  mA, at fixed radial distance (1.7 cm), and (1 cm) for probes 1, 3 and 2 respectively.

## 5.2 Double Probe Characteristics at Constant Pressure (0.7 torr) and Different Distances from The Axis:

### 5.2.1 Current-Voltage Characteristics:

Radial diffusion of electrons and ions is a key ingredient of the Schottky theory. Since the Debye length is small compared with the tube diameter, the discharge is assumed to exhibit approximate local charge neutrality. In addition, all recombination is assumed to occur on the wall, where the electron density is assumed to approach zero. According to the theory of ambipolar diffusion, a radial electric field is established which retards the diffusion of electrons to the wall, and accelerates the diffusion of ions so as to make their diffusive fluxes equal.

The I-V characteristic at constant pressure and different radial position of the probe can be seen in Figs.( 5.8 and 5.9). It has been shown that the ion random current increases as the probe move towards the axis (or decreases by increases the radial distance from the axis).



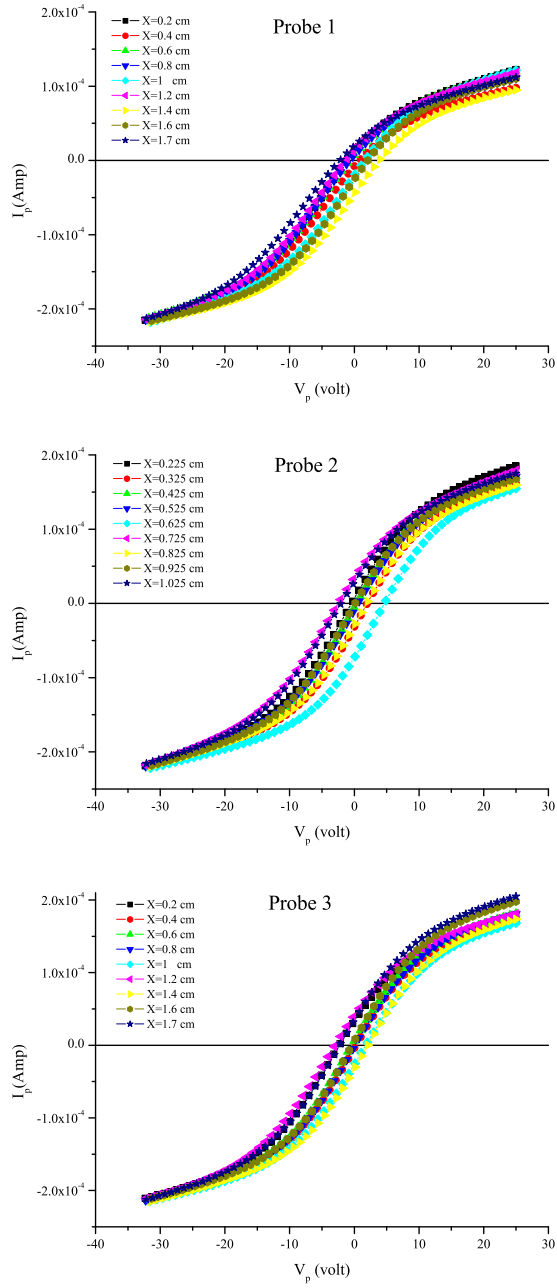


Figure 5.8: Double probe characteristic in argon gas at  $I_d = 5$  mA at constant pressure ( $p = 0.7$  torr) and different distances.

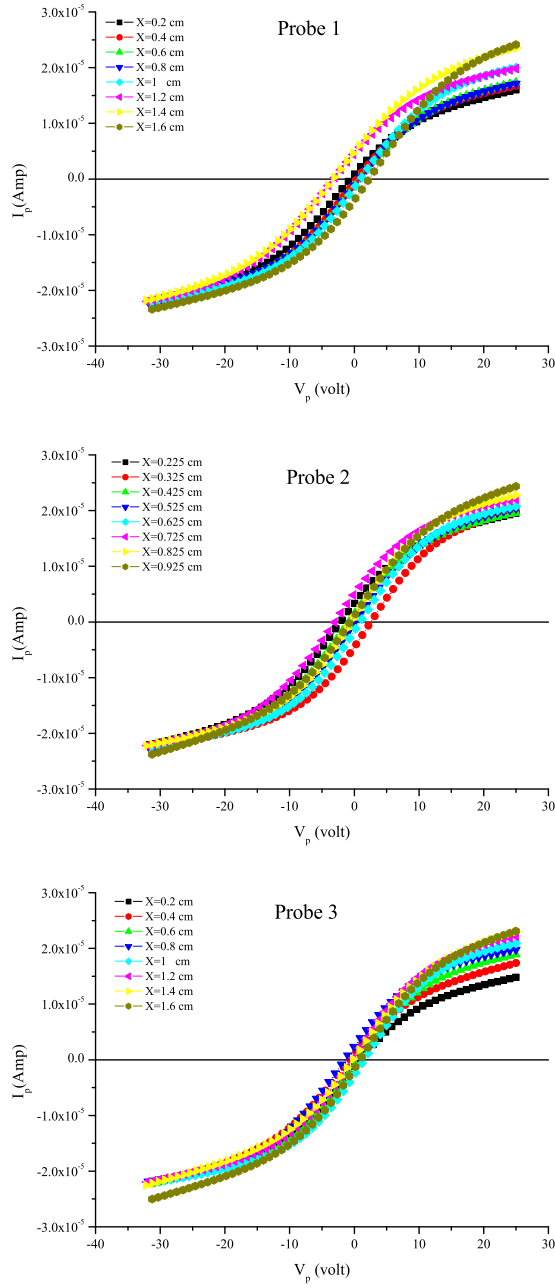


Figure 5.9: Double probe characteristic in argon gas at  $I_d = 15$  mA at constant pressure ( $p = 0.7$  torr) and different distances.

### 5.2.2 The Electron Temperature and Density:

Figs.( 5.10 and 5.11) illustrate the electron temperature  $T_e$  and density  $n_e$  profiles as a function of various radial positions at constant pressure 0.7 torr. The influence of the plasma tube dimensions on the plasma parameter profiles are rather modest; a weak contraction of the profiles are observed as the tube radius increases. The axial variation shows a peak in the center decreasing as the sheath is approached. The probe measurements will be greatly perturbed when the tips enter the sheath region.

Fig.( 5.10) shows that the electron temperature at the center for all regions has a maximum value, and its value at the first region, probe1, is greater than that of the other regions, at probes2 and 3. Since we are in the transition region, Faraday space, where the electron density  $n_e$  decreases from high values in the negative glow to lower values in the positive column, therefore the electron temperature and axial electric field increases in the opposite direction[50]. However, as can be seen from Fig.( 5.11), the electron density  $n_e$  at probe2, at low discharge currents, have higher values than that of probe3. This can be explained as follows: Since the most important parameter in spatial distribution of the charged particles is the ratio of the diffusion length (or the mean free path) to the gradient length of the plasma distribution  $\lambda/L_D$ , then as this value decreases, the spatial variation of the electron and argon ion densities increase. In general, this value is inversely proportional with the discharge tube radius. Therefore, at large radii, there is a

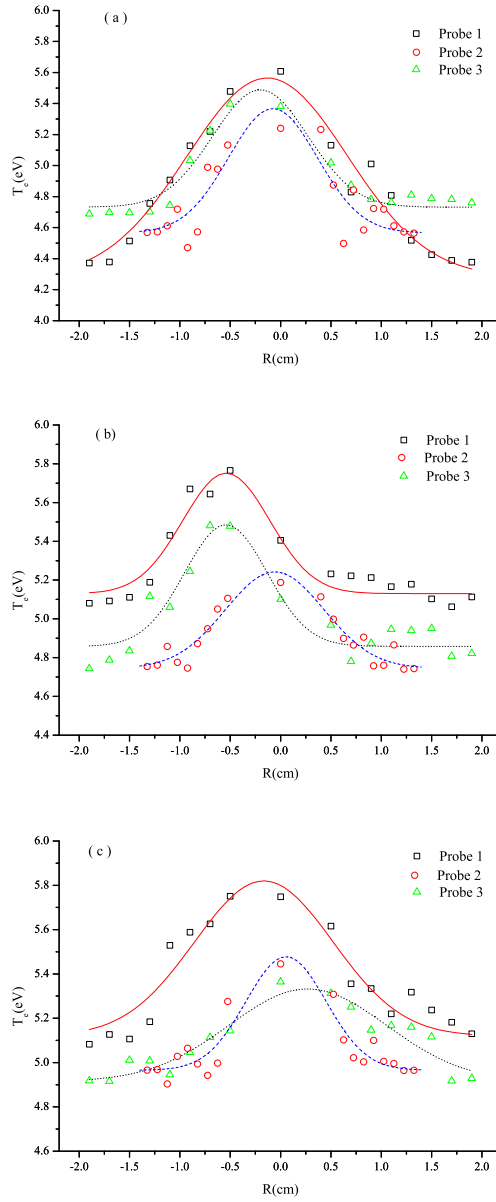


Figure 5.10: Electron temperature as a function of the different radial distance  $R$  at discharge current (a)  $I_d = 5$  mA, (b)  $I_d = 10$  mA, and (c)  $I_d = 15$  mA, at  $P = 0.7$  torr. The experimental (symbols) and theoretical (lines) curves for probes (1-continuous, 2-dash, and 3- dots, for all figures).

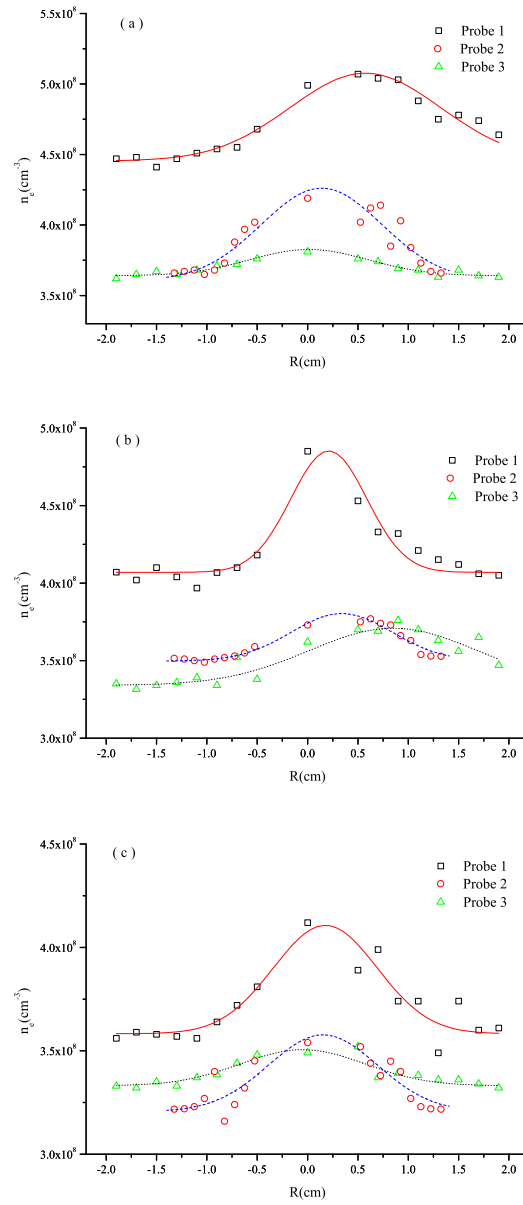


Figure 5.11: Electron density as a function of the different radial distance  $R$  at discharge current (a)  $I_d = 5$  mA, (b)  $I_d = 10$  mA, and (c)  $I_d = 15$  mA, at  $P = 0.7$  torr.

net loss of electrons near the axis and the electron density decreases there[45, 51]. Hence, we have higher electron temperature at probe3 than at probe2. Decreasing of the electron temperature in the radial direction is a result of motion of the electrons and ions obeying to the ambipolar diffusion. From the previous work of the constant radius cylindrical discharge tube systems[4, 9, 50, 52, 53], it has been shown that the electron temperature increases from the cathode up to the distance 2.5 cm (the edge of the negative glow), where the maximum value is observed, then it decreases from the leading edge of the negative glow up to the distance 4.5 cm, and stay approximately constant up to the anode. In other words, if we take the relation between the Faraday space and the radius of the discharge tube under consideration, Faraday space will be stopped at  $x \approx 4 - 6$  cm for  $R = 1.4$  cm and longer, about  $x \approx 8 - 10$  cm for a radius of  $R = 5$  cm. Therefore, in our discharge system, the positive column starts after probe1, and the variation of the plasma parameters is not like the traditional one that has a constant radius with constant electron density, electron temperature, and axial electric field[35].

On the other hand, when the discharge current increased at constant pressure; the radial distribution of the electron density and temperature are approximately remaining close to the typical profile of the fundamental diffusion (zero order Bessel function  $J_0(2.405/R)$ ), with a little narrower profile than the classical one. For all discharge currents, the electron temperatures have higher values in the

Faraday space region with relatively lower temperatures in the positive column region. Generally, increasing the discharge current lead to increase (decrease) in the electron temperature (density) and make Faraday space, at probe1, shorter with lower electron density. For the higher discharge currents  $I_d = 15$  mA, it is observed that the  $T_e$  at probe2 has higher values than that of probe3. Since a smaller tube diameter causes an increase in ambipolar diffusion to the walls, a higher electron temperature and electric field to maintain the ionization is required, as can be seen from Figs.5.10(c). This observation is also supported by references [54, 55, 56].

### 5.2.3 The Floating Potential (Radial Potential):

Another important magnitude in the plasma diagnostics is the floating potential  $V_f$  for which the net current collected by the probe immersed in the plasma is zero. The radial variation of the floating potential measured with (TCDP) is shown in Fig. 5.12. The value of  $V_f$  is relatively small near the axis, but increases to larger values near the wall. This is due to the development of the plasma sheath near the wall.

The floating potential may depend on the drift velocity  $v_d$  of the bulk plasma ( $v_d = v_e/v_{th}$ ), where  $v_e$  is the electron drift velocity, and  $v_{th}$  is the thermal velocity of electron, and the range of variation of the floating potential becomes

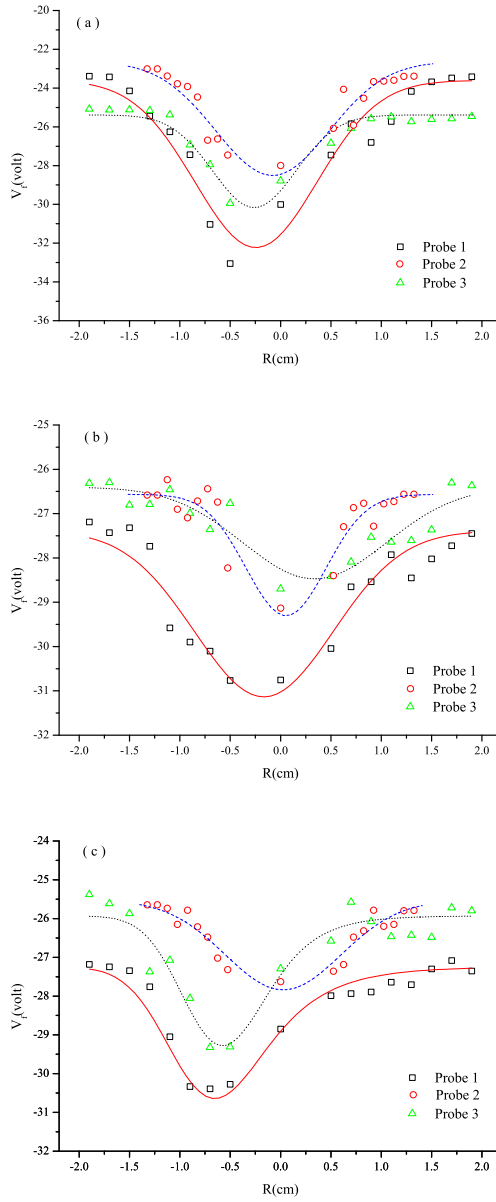


Figure 5.12: Floating potential as a function of the different radial distance  $R$  at discharge current (a)  $I_d = 5$  mA, (b)  $I_d = 10$  mA, and (c)  $I_d = 15$  mA, at  $P = 0.7$  torr.



larger by increasing the electron drift velocity. Therefore, as the electron temperature increased, the  $V_f$  becomes more negative[57, 58]. Therefore, the  $V_f$  has less negative value at the probe2 for all discharge conditions except at  $I_d = 15$  mA.

#### 5.2.4 The Normalized Probe Radius $\xi = r_P/\lambda_D$ :

Figs.( 5.13 - 5.15) shows the relation between the electron temperatures, densities, and  $\xi$  for (TCDP) at different discharge currents, at constant pressure 0.7 torr. The behavior of  $T_e$  are almost the same for all three regions, but the values of  $n_e$  differ by an amount which increases with  $\xi$ . However, at low density region ( probe3 ), the value of  $\xi$  approximately remain constant as shown in Figs.( 5.13 and 5.15) at discharge currents (5 and 15 mA) for probe3, and at probe2 at  $I_d = 10$  mA. According to[37, 59] the ion current depends on the normalized probe radius ( $\xi = r_p/\lambda_D$ ). When  $\xi$  is small, the  $n_e$  is small , incoming ions are crowded together and form a large positive space charge near the probe surface. This space charge creates an electric field, driving the ions out past the end of the probe. Since  $\xi < 1$ , the sheath is assumed to have a distinct boundary which is independent of the probe bias voltage. In addition, if  $T_e \gg T_i$ , the sheath boundary will be distinct because the ions will all be reflected when there is a potential increase small compared to the electron temperature.

The validity of this technique has been verified in term of  $\lambda_D$  and  $\xi$ , and it is observed that  $\xi$  has a value around 0.1. Also, the mean-free path of the electrons

and ions is large compared to the sheath dimensions[29].

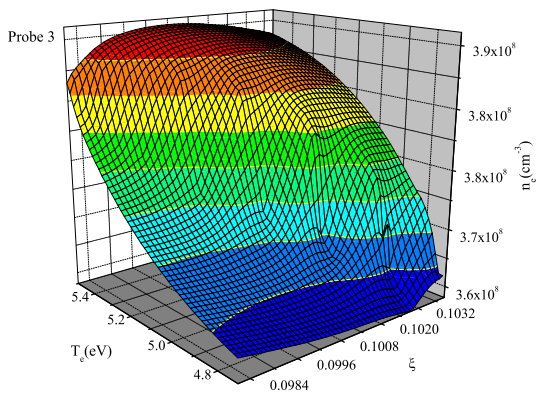
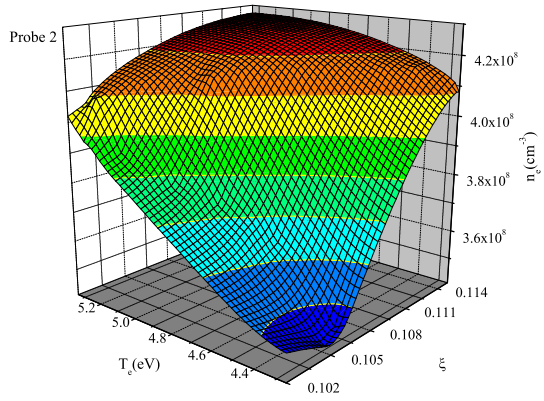
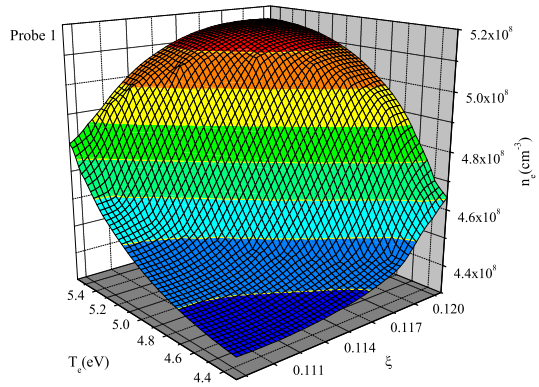


Figure 5.13: Radial variation of normalized probe radius  $\xi$  as a function of electron temperature and density at discharge current  $I_d = 5$  mA, and  $P = 0.7$  torr.

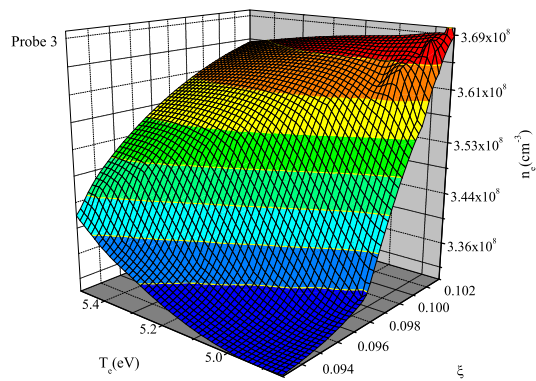
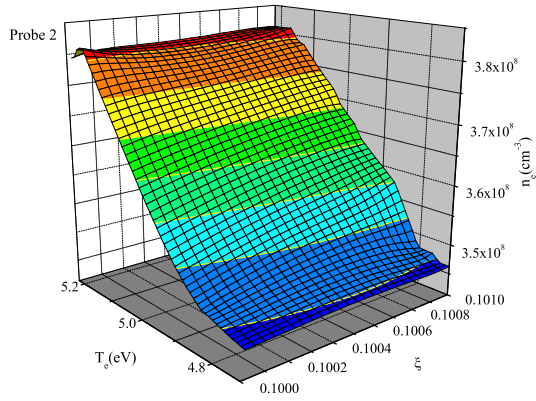
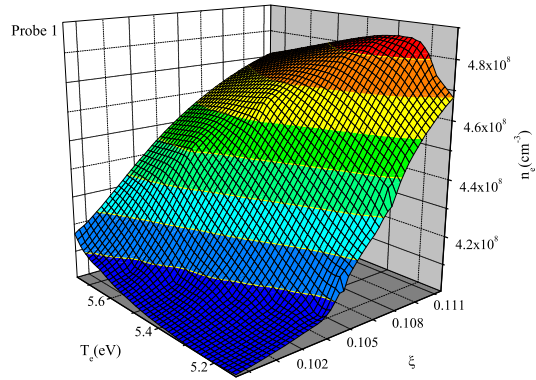


Figure 5.14: Radial variation of normalized probe radius  $\xi$  as a function of electron temperature and density at discharge current  $I_d = 10$  mA, and  $P = 0.7$  torr.

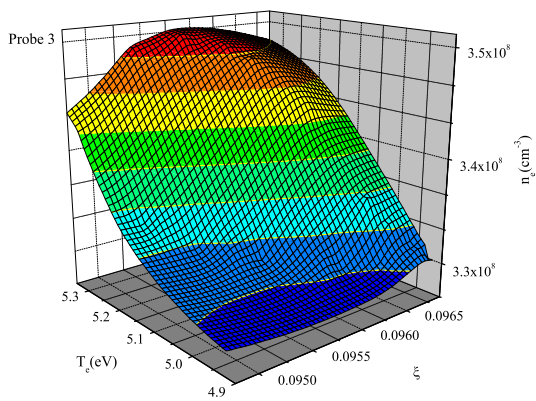
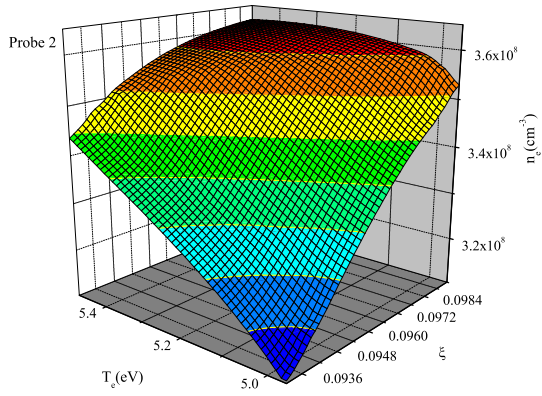
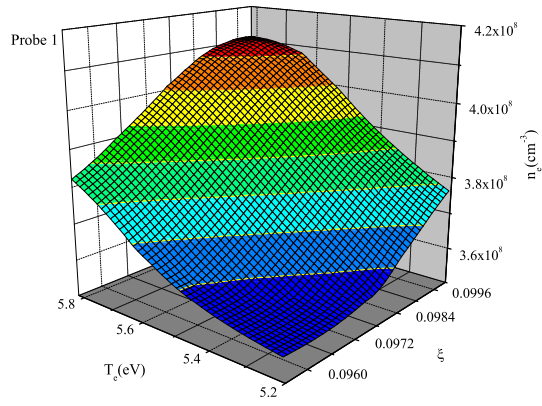


Figure 5.15: Radial variation of normalized probe radius  $\xi$  as a function of electron temperature and density at discharge current  $I_d = 15$  mA, and  $P = 0.7$  torr.

## CHAPTER 6

### CONCLUSION AND FUTURE WORKS

#### 6.1 Conclusion

The non-uniform positive column argon dc glow discharge plasma has been investigated experimentally. To measure all plasma parameters, the computerized three dual Langmuir probe array set-up has been used with optically isolated circuit. This is to prevent stray capacitance to ground which can be a major source of error at the turn-on and turn-off transients. With 10 kHz low-pass filters a very good resolution and accuracy have been measured, and give a possibility to use it in a magnetized plasma and low frequency oscillating plasma systems. The results show that:

##### 6.1.1 Conclusion For Axial Measurements

1- The current-voltage characteristic has been shifted toward the negative direction with increasing the pressure, and the probe current in the double probe technique decreases with the increasing  $pR$ .

2- The I-V characteristic increases by increasing discharge current due to the

density of atoms in the ground-state and the availability of a depletion of ground-state atoms near the axis.

3- The electron temperature and axial electric field decreases, and electron density increases with  $pR$ , and they remain constant with discharge current; except  $T_{e1}(n_{e1})$  decreases (increases). However, the effect of variable radii system leads to get unexpected results. The small radius caused to increase the density and decrease of the electron temperature and electric field, which is also encountered in ref.[4], due to the electron-electron collision domination. Therefore, the uniformity of the positive column has been changed, but with approximate electrical neutrality.

4-The axial electric field tend to decrease very slowly with rising pressure according to the interrelation of the electron temperature and the axial electric field which is in agreement with the ambipolar diffusion theory.

Table 6.1 summarizes all changes in electron temperatures, electron densities, and axial electric fields for all probes at different discharge currents.

Table 6.1: Electron temperatures  $T_e$ , electron densities  $n_e$ , and axial electric field  $E$  for all probes at different discharge currents. Note: numbers (1, 2, 3) refers to probe1, probe2, and probe3 respectively.

$I_d=5(\text{mA})$	$I_d=10(\text{mA})$	$I_d=15(\text{mA})$
$T_{e1} > T_{e3} > T_{e2}$	$T_{e1} > T_{e3} > T_{e2}$	$T_{e1} \approx T_{e3} > T_{e2}$
No change	At low pressures: No change	$T_{e3} > T_{e1} > T_{e2}$
$n_{e2} > n_{e3} > n_{e1}$	$n_{e1} \approx n_{e2} > n_{e3}$	$n_{e1} > n_{e2} > n_{e3}$
No change	At low pressures: $n_{e3} > n_{e2} > n_{e1}$	$n_{e2} > n_{e1} > n_{e3}$
$E_{e1} > E_{e3} > E_{e2}$	$E_{e1} > E_{e3} > E_{e2}$	$E_{e1} \approx E_{e3} > E_{e2}$
$E_{e1} > E_{e2} > E_{e3}$	At low pressures: No change	No change

### 6.1.2 Conclusion For Radial Measurements

1- Moving both side of each double probe at the same time may give not accurate local plasma parameter measurements, due to the increasing the distance between each probe.

2- It has been shown that the ion random current increases as the probe move towards the axis (or decreases by increases the radial distance from the axis).

3- The radial electron temperature and density have the maximum value at the column axis where the electrostatic potential is the highest. A range ( $10^8 \text{ cm}^{-3}$ ) of plasma densities permitted studies with probe sheath that was thick compared to the probe radius. It was observed that the radial  $T_e$  decreases, at low  $I_d$ , and  $n_e$  increases with decreasing discharge tube radius. However, at higher discharge current  $T_e$  may increase somewhat and be higher than the  $T_e$  at the right region



(near the anode ).

4- Furthermore, the  $\xi$  is proportional to the electron density for a given value of  $T_e$ , and remain constant if the ratio between increasing value of  $T_e$  is equal to the decreasing value of  $n_e$ .

## 6.2 Future Works

1- Developing the measurement technique to be more fast and more electronically controlled. For example, using programmable switches to control the gains.

2- Using uniform magnetic coils to confine plasma to get a high density plasma and reduce the loss energy.

3- Using magnetic coils to get a (Cusp Plasma).

4- Using different gases and its mixtures.

5- Using  $RF$  power instead DC power to get  $RF$  plasma.

6- Using conducting metallic wall instead of glass wall to study the plasma wall inter-action.

## REFERENCES

- [1] National Research Council, Panel on Opportunities(Author).Plasma Science:From Fundamental Research to Technological Applications. Washington, DC, USA: National Academies Press, (1995).
- [2] National Research Council Staff(Author). Plasma Processing of Materials : Scientific Opportunities and Technological Challenges. Washington, DC, USA: National Academy Press, (1991).
- [3] F. F. Chen, Plasma Diagnostic Techniques, Academic Press INC., New York, (1965).
- [4] Yuri P. Raizer, Gaz Discharge Physics, Spring Verlag, (1987).
- [5] J. Smith, IEEE Trans. Electron Devices ED-20, 1103, (1973).
- [6] Y. Okamoto, Japan. J. Appl. Phys. 15, 719,(1976).
- [7] T. Kaneda, J. Phys. D: Appl. Phys. 23, 500, (1989).
- [8] C. Wilke, B. P. Koch, and B. Bruhn, Physics of Plasmas 12, 3350, (2005).
- [9] W. Tao, and H. K. Yasuda, Plasma chem. and Plasma Processing 22, 297, (2002).
- [10] E. Hintz, 3rd Workshop on Plasma and Laser Technology, Ismailia, (1993).
- [11] C. M. Anderson, W. G. Graham, and M. B. Hopkins, Appl. Phys. Lett. 52, 783, (1988).
- [12] A. Von Engel, Ionized Gaz, Oxford:Oxford University Press, (1965).
- [13] J. D. Cobine, Gaseous Conductors ,Theory and Engineering Application, Dover Publications Inc., New York, 2nd edition, (1958).
- [14] R. N. Franklin, Plasma Phenomena In Gas Discharges, Clarendon Press. Oxford,(1976).
- [15] D. Akbar, and S. Bilikmen, Development of Computer Controlled Double Probe and Discharge System with Varying Diameters, 14th International Conference on Surface Modification of Materials by Ion Beams (SMMIB), Kusadasi, Turkey, 04 Sept. 2005.

- [16] D. Akbar, and S. Bilikmen, Fast Double Probe Technique and Effect of Non-Uniform Glow Discharge System on Plasma Parameters, 23th International Physics Congress (TPS), Mugla, Turkey, 13-16 Sept. 2005.
- [17] W. Schottky, Z. Phys. 25, 635, (1924).
- [18] Ingold J H 1997 Phys. Rev. E. 56 5932.
- [19] Loffhagen D , and Gorchakov S 2005 "Self-consistent Modelling of the Column Plasma of Low-pressure Glow Discharges", *XXVII<sup>th</sup>* ICPIG, Eindhoven, the Netherland, July 18-22.
- [20] A. V. Pheleps, and S.C. Brown, Phys. Rev. 13, 1202, (1952).
- [21] H. J. Oskan, Philips Res. Rep. 13, 335, (1958).
- [22] J. P. Graur, and L. M. Chainin, Phys. Rev. 182, 167, (1969).
- [23] Y. Ichikawa, and S. Teii, J. Phys. D:Appl. Phys. 13, 2031, (1980).
- [24] P. M. Chung, L. talbot, and K. J. Touryan, *Electrostatic Probes in Stationary and Flowing Plasmas*, Springer-Verlag, New York, (1975).
- [25] J. D. Swift, and M. J. R. Schwer, *Electrical Probes for Plasma Diagnostics*, American Elsevier, New York, (1969).
- [26] H. M. Mott-Smith, and I. Langmuir, Phys. Rev. 28, 727, (1929).
- [27] F. F. Chen, Phys. Plasma 8, 3029, (2001).
- [28] J. E. Allen, Phys. Scr. 45, 497, (1992).
- [29] J. H. Rogers, J. S. De Groot, and D. Q. Hwang, Rev. Sci. Instrum. 63, 31, (1992).
- [30] F. F. Chen, Langmuir Probe Diagnostics, Mini-Course on Plasma Diagnostics, IEEE-ICOPS meeting, Jeju, KOrea, (2003).
- [31] E.O. Johnson, and L. Malter, Phys. Rev. 80, 58, (1950).
- [32] J.R. Cozens, and A. Von Engle, Int. J. Electron 19, 61, (1965).
- [33] D. Bardley, and K. J. Mathews, Phys. Fluids 10, 1336, (1967).
- [34] B. A. Smith, and L. J. Oreizet, Plasma Source. Sci. Technol. 8, 82, (1999).
- [35] D. Akbar, and S. Bilikmen, J. Appl. Phys. D: Appl. Phys. (2006)(submitted). s

- [36] D. S. Isaac , and W. R. Claude , J. Appl. Phys. 76, 4488, (1994).
- [37] Francis F. Chen, John D. Evans, and Arnush, D., Phys. Plasmas 9, 1449, (2002).
- [38] L. S. Pilling, E. L. Bydder, and D. A. Carnegie, Rev. Sci. Instrum. 74, 3341 (2003).
- [39] D. Akbar, Experimental Study of Plasma Parameters in Air and Nitrogen Glow Discharge Using Probe Technique, M.Sc. Thesis, Mosul University, Iraq, (1996).
- [40] A. G. Mathewson, A. Grillot, and S. Hazeltine, Vacuum 31, 337, (1981).
- [41] T. M. Desai, S. V. Gorwale, and Shukla, Vacuum 46, 223, (1995).
- [42] G. Alferd, Cold Plasma in Material Fabrication:from fundamentals to applications, IEEE Press , New York, (2002).
- [43] T. Kaneda, J. Phys. D: Appl. Phys. 12, 61, (1979).
- [44] T. Dote and T. Kaneda, Jap. J. Appl. Phys. 15, 1399, (1976).
- [45] D. Uhrlandt, J. Phys. D: Appl. Phys. 35, 2159 (2002).
- [46] N. Bashlov et al, J. Phys. D:Appl. Phys. 31, 1449, (1998).
- [47] D. A. Herman, D. S. McFarlane, and A. D. Gallimare, the 28th International Electronic Propulsion Conference, Toulouse, France, (2003).
- [48] M. Tuszewski, and J. A. Tobin, Plasma Sources Sci. Technol. 5, 640, (1996).
- [49] D. Akbar, and S. Bilikmen, Chinese. Phys. Letter (Accepted, Vol 23 No.5 2006).
- [50] Yu. M. Kagan, C. Cohen, and P. Avivi, J. Appl. Phys. 63, 60 (1988).
- [51] M. J. McCaughey, and M. J. Kushner, J. Appl. Phys. 69, 6952 (1991).
- [52] T. Kimura, K. Akatsuka, and K. Ohe, J. Appl. Phys.D:Appl. Phys. 27, 1664 (1994).
- [53] W. H. Tao, M. A. Prelas, and H. K. Yasuda, J. Vac. Sci. Technol. A 14, 2113 (1996).
- [54] T. B. Read, Brit. J. Appl. Phys. 14, 36 (1963).
- [55] G. A. Hebner, J. Appl. Phys. 80, 2624 (1996).

- [56] Z. Liu, D. Lui, and C. Ning, *Vacuum* 44, 1041 (1993).
- [57] G. Pertraconi, and H. S. Maciel, *Barazilian J. Phys.* 33, 782 (2003).
- [58] Cheol-Hee Nam, N. Hershkowitz, *J. Appl. Phys.* 63, 5674 (1988).
- [59] P. Spanel, M. Tichy, D. Smith, O. Chudacek, and P. Kudrna, *Contrib. Plasma Phys.* 35, 3, (1995).

## VITA

### PERSONAL INFORMATION

Surname, Name: Akbar, Demiral  
Date and Place of Birth: 05 October 1970, Kerkuk, IRAQ.  
e- mail: akbar@metu.edu.tr

### EDUCATION

Degree	Institution
M.Sc.	Mosul University (1996), Mosul, IRAQ.
B.Sc.	Mosul University (1994), Mosul, IRAQ.
High School	Al-Valid High School, Kerkuk, IRAQ.

### REWARDS

-1993 1<sup>st</sup> of Physics Department (IRAQ).  
-2005 Graduate Student Award for Outstanding Research Contributions, 14<sup>th</sup>  
SMMIB (TURKEY).

## PUBLICATION LIST

- 1- D. Akbar, and S. Bilikmen, Development of Computer Controlled Double Probe and Discharge System with Varying Diameters, 14th International Conference on Surface Modification of Materials by Ion Beams (SMMIB), Kusadasi, Turkey, 04 Sept. 2005.
- 2- D. Akbar, and S. Bilikmen, Fast Double Probe Technique and Effect of Non-Uniform Glow Discharge System on Plasma Parameters, 23th International Physics Congress (TPS), Mugla, Turkey, 13-16 Sept. 2005.
- 3- D. Akbar, and S. Bilikmen, Chinese. Phys. Letter (Accepted, Vol 23 No.5 2006).
- 4- D. Akbar, and S. Bilikmen, J. Appl. Phys. D: Appl. Phys. (2006)(submitted).